# Novel roles for phospholipase C in plant stress signalling and development

Zhang, Q.

**Publication date**
2017
**Document Version**
Other version
**License**
Other

# Chapter 4

## Role for Arabidopsis *PLC7* in stomatal closure, mucilage adherence, and leaf serration

Qianqian Zhang,[1,2] Ringo van Wijk,[1,2] Mart Lamers,[1,*] Francisca Reyes Maarquez,[3] Aisha Guardia, [4] Denise Scuffi, [4] Carlos García-Mata,[4] Wilco Ligterink,[3] Michel A. Haring,[1] Ana M. Laxalt,[4] & Teun Munnik[1,2]

*[1]Section Plant Physiology or [2]Plant Cell Biology, Swammerdam Institute for Life Sciences, University of Amsterdam, Science Park 904, Amsterdam, 1098 XH, The Netherlands, [3]Lab. of Plant Physiology, Wageningen University, Droevendaalsesteeg 1, 6708 PB, Wageningen, The Netherlands, [4]Instituto de Investigaciones Biológicas (IIB-CONICET-UNMdP), Universidad Nacional de Mar del Plata, Mar del Plata, Argentina.*

**ABSTRACT**

**Phospholipase C (PLC) signaling in plants is likely different from the well-established animal paradigm as the prime targets for $IP_3$ and DAG are absent, and plants contains very small amounts of the putative PLC substrate, phosphatidylinositol 4,5-bisphosphate ($PIP_2$). Nonetheless, the genome of *Arabidopsis thaliana* encodes 9 *PLC* genes. To increase our understanding of PLC signaling in plants, we have started to analyze various knock-out (KO), knock-down (KD) and overexpression lines of Arabidopsis. Here, we functionally characterized Arabidopsis *PLC7.* Promoter-GUS analyses revealed that *PLC7* is specifically expressed in the phloem of roots, leaves and flowers and also in trichomes and hydathodes. Two T-DNA insertion mutants were obtained, with *plc7-3* being a KO- and *plc7-4* a KD line. In contrast to earlier-characterized phloem-expressed *PLC* mutants, *plc3* and *plc5*, *plc7* mutants revealed no defects in primary- or lateral root development. Nonetheless, like *plc3* mutants, *plc7* mutants were found to exhibit a reduced sensitivity to ABA during stomatal closure. Double-knockout *plc3 plc7* lines were found to be lethal, whereas *plc5 plc7 (plc5/7)* mutants were viable, and revealed several new phenotypes, not observed earlier in the single mutants. These include a defect in seed mucilage, enhanced leaf serration, and an increased tolerance to drought. *PLC7* overexpression lines showed an enhanced drought tolerance, similar to what was found for *PLC3* and *PLC5* overexpression lines. *In vivo* $^{32}P_i$-labeling of seedlings treated with sorbitol, to mimic drought stress, revealed increased $PIP_2$ responses in both drought tolerant *plc5/7* and *PLC7-OE* mutants. Together, these results reveal several novel functions for *PLCs* in plant stress and development. Potential mechanisms for this are discussed.**

*Key words: PLC*; seed mucilage; leaf serration; ABA sensitivity; drought tolerance.

## INTRODUCTION

Phospholipase C (PLC) plays a key role in mammalian signal transduction. Its intracellular activation through transmembrane receptor occupation leads to the hydrolysis of phosphatidylinositol 4,5-bisphosphate ($PIP_2$) to produce two second messengers, inositol 1,4,5- trisphosphate ($IP_3$) and diacylglycerol (DAG). $IP_3$ triggers the release of $Ca^{2+}$ from an intracellular store via ligand-gated $Ca^{2+}$ channel, while DAG recruits and activates protein kinase C (PKC) and stimulates TRP- (transient receptor potential-) channels. The subsequent increase in $Ca^{2+}$ and change in phosphorylation status of numerous targets regulates multiple cellular processes that orchestrate the cell's response to the initial stimulus (Irvine, 2006; Michell, 2008; Balla, 2013).

The PLC signaling pathway in plants is still enigmatic (Munnik, 2014). While higher plant genomes encode all genes required for the metabolism of this pathway, they all lack the prime targets for $IP_3$ and DAG, i.e. the $IP_3$ receptor, PKC and TRP channels (Wheeler and Brownlee, 2008; Munnik and Testerink, 2009; Munnik and Vermeer, 2010; Munnik and Nielsen, 2011; Munnik, 2014; Heilmann, 2016). Instead, plants seem to phosphorylate $IP_3$ and DAG into inositolpolyphosphates (IPPs) and phosphatidic acid (PA), respectively, which are believed to function as second messengers (Gillaspy, 2013; Munnik, 2014; Heilmann, 2016). $IP_3$ was initially thought to release $Ca^{2+}$ from intracellular stores when microinjected (Gilroy et al., 1990; Blatt et al., 1990; Allen and Sanders, 1994; Hunt and Gray, 2001), but later it was shown that this $IP_3$ is phosphorylated to $IP_6$ within seconds, and that the latter compound was 10-100 fold more effective in releasing $Ca^{2+}$ (Lemtiri-Chlieh et al., 2000, 2003). Meanwhile, various other signaling functions for $IP_6$ and other IPPs have been emerging, including the pyro-phosphorylated $IP_7$ and $IP_8$. In yeast and mammalian cells, these IPP molecules play important roles in various nuclear processes, including gene transcription, chromatin remodeling, mRNA export and DNA repair, and are involved in a wide range of cellular processes, including osmoregulation, phosphate homeostasis, vesicular trafficking, apoptosis, insulin- and immune signaling, cell cycle regulation, and ribosome synthesis(Monserrate and York, 2010; Thota and Bhandari, 2015; Williams *et al.*, 2015). In plants, besides releasing $Ca^{2+}$ in guard cells, $IP_6$ has also been shown to bind the auxin receptor, TIR1 (Tan *et al.*, 2007), which is proposed to functionally regulate the $SCF^{TIR1}$ ubiquitin-ligase complex to control downstream auxin mediated-gene expression (Chapter 2; Chapter 3; Zhang et al., 2017). Similarly, COI1, the receptor for jasmonate signaling was found to bind $IP_5$ (Sheard *et al.*, 2010), with functional significance for plant immunity(Mosblech *et al.*, 2008, 2011; Murphy *et al.*, 2008), even though it could be that the pyrophosphorylated form of $IP_5$, i.e. PP-$IP_5$ (= $IP_7$), is biologically responsible for this (Laha *et al.*, 2015, 2016). GLE1, an mRNA export factor, was recently identified as an important $IP_6$ target in Arabidopsis involved in $P_i$ homeostasis (Lee *et al.*, 2015). SPX domain-containing proteins have recently been identified to bind IPPs, including $IP_6$ and many of these proteins are involved in $P_i$ signaling (Kuo *et al.*, 2014; Puga *et al.*, 2014; Wild *et al.*, 2016). For PA, several plant targets have been identified over the years, including protein kinases, proteins

phosphatases, small G-proteins, RBOH (NADPH oxidase), GAPDH, ion channels and actin-binding proteins (Wang *et al.*, 2006; Mosblech *et al.*, 2011), and PA has been implicated to regulate many cellular processes, including vesicular trafficking, cytoskeleton dynamics, and ion-channel regulation (Li *et al.*, 2009, 2012, Pleskot *et al.*, 2010, 2017; Testerink and Munnik, 2011; Thomas and Staiger, 2014). Note that PA is not only generated via PLC and DAG kinase (DGK), it can also be indirectly formed via other DAG-generating enzymes, like non-specific PLCs (NPC; Munnik, 2014), or directly, through phospholipase D (PLD) hydrolysis of structural phospholipids (Wang *et al.*, 2006; Li *et al.*, 2009; Liu *et al.*, 2013).

How, when, and whether PLC signaling is involved in generating PA and IPPs in the above events is still largely unknown and mostly based on correlations and indirect evidence. Hence, tools to genetically manipulate *PLC* levels will be very helpful to functional characterize its role(s). In this way, silencing of *PLC* revealed its importance in plant defense in tomato and Arabidopsis (Vossen *et al.*, 2010; D'Ambrosio *et al.*, 2017), in cytokines- and gravity signaling in *Physcomitrella* (Repp *et al.*, 2004), in ABA signaling and stomatal control in tobacco and Arabidopsis (Sanchez and Chua, 2001; Hunt et al., 2003) but also in development, where Arabidopsis *PLC2* plays a key role in gametogenesis, reproduction and root development (Li et al., 2015; Laxalt et al., 2016; R. van Wijk and T. Munnik, In prep.). In petunia and tobacco, PLC regulates pollen tube-tip growth (Dowd *et al.*, 2006; Helling *et al.*, 2006). Alternatively, several Arabidopsis T-DNA insertion mutants have meanwhile revealed several roles for *PLC3*, *PLC5* and *PLC9* in seed germination, (lateral) root development, ABA signaling and heat stress tolerance ( Chapter 2 and 3; Zheng *et al.*, 2012; Gao *et al.*, 2014). On the other hand, overexpression of *PLC* has been shown to increase drought tolerance in maize, canola, tobacco and Arabidopsis (Wang et al., 2008; Georges et al., 2009; Tripathy et al., 2011; Chapter 2 and 3). Even though it is still unknown how PLC exactly achieves all the above, it is very important that these molecular tools become available for physiological and biochemical studies.

The Arabidopsis genome encodes 9 *PLC* genes, which are subdivided into four clades (Hunt et al. 2004; Tasma et al., 2008; Pokotylo et al., 2014). Earlier, we found that knock-out (KO) mutants of *PLC3* or a knock-down (KD) mutant of *PLC5*, exhibited small defects in root development, i.e. 5-10% reduced growth of the primary root and a 10-20% reduction in the number of lateral roots. Interestingly, even though these *PLCs* come from different subfamilies, *plc3 plc5*-double mutants did not intensify the phenotype, indicating other *PLCs* could be involved. Since *PLC3* and *PLC5* were specifically expressed in phloem-companion cells and revealed a segmented expression pattern in the root form which lateral roots emerged, we search for other Arabidopsis *PLCs* specially expressed in the phloem, and found *PLC7*. This gene belongs to a different subfamily than *PLC3* and *PLC5*. Promotor-GUS analyses confirmed its expression in all vascular tissues, but also in trichomes and hydatodes, however *plc7-3* KO- or *plc7-4* KD mutants revealed no defects in root or shoot development. Creating double mutants revealed that the combination *plc3/7* was lethal and that *plc5/7* did not exhibit defects in root development either. Nonetheless, several new phenotypes appeared for the latter mutant, including non-

adherent mucilage, enhanced leaf serration and increased drought resistance. In addition, like *PLC3* and *PLC5*, overexpression of *PLC7* also leads to an increase in drought tolerance.

## RESULTS

### Expression of *PLC7* during plant development

Histochemical assays on *pPLC7-GUS-SYFP* reporter lines indicated that *PLC7* was mainly expressed in the vasculature throughout all developmental stages, including root, cotyledons, leaves, hypocotyl, flower (stamen, style, petal, sepal, receptacle and pedicel) and silique septum (Fig. 1a-j, n and o), which is similar to the expression pattern of *PLC3* (Zhang et al, 2017; Chapter 2) and *PLC5* (Chapter 3). However, there are also some differences. During seed germination *PLC7* expression was mainly observed in the hypocotyl (28h after transfer to 22ºC, Fig. 1a), which remained like this in 2-day old seedlings (Fig. 1b) and then spread to the vasculature throughout the plant upon further development (Fig. 1c-j). Interestingly, *GUS* expression was quite abundant in hydathodes, in young seedling, but also mature plants (Fig. 1b-e, l, arrows). Unlike *PLC3* and *PLC5*, *PLC7* did not display the characteristic, segmented expression in the root vasculature. Instead, expression was homogenous in both main root- and lateral root vasculature (Fig. 1f, g). The expression stopped near the transition zone of the root (Fig. 1h). Strong GUS staining was visible in trichomes (Fig. 1j, k), which is similar to that of *PLC5*, but stronger and different from *PLC3,* that is only expressed in trichome basal cells. No GUS activity was detected in guard cells, as was found for *pPLC3::GUS-YFP* and *pPLC5::GUS*. These results confirm that *PLC7* is expressed throughout the plant (Tasma *et al.*, 2008), but the expression is mostly restricted to the vasculature.

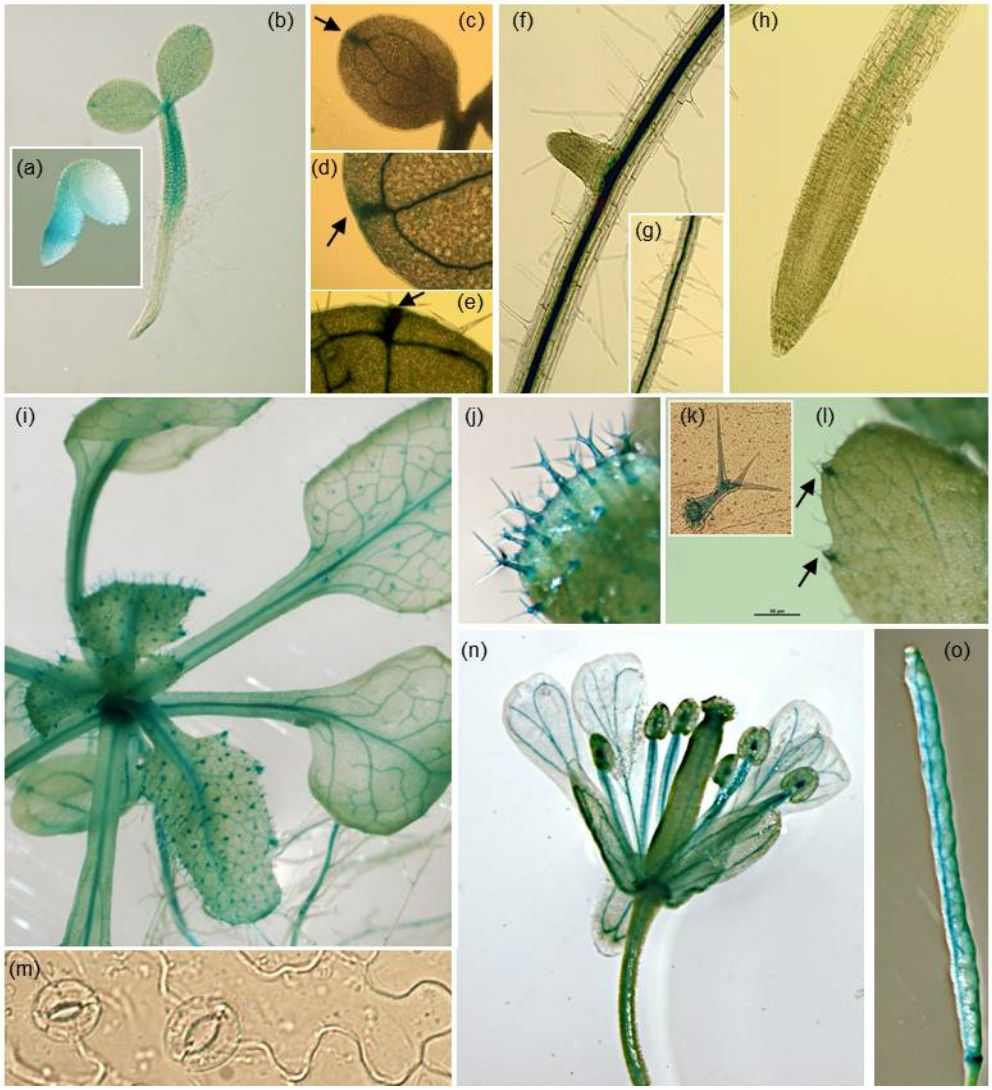


**Figure 1.** *pPLC7::GUS-SYFP* expression in seedlings and mature tissues of Arabidopsis.
GUS staining was found in: Embryo, 28 hrs after stratification (a), vascular tissue of 2-d old seedlings (b) and in 10-d old seedlings, including, cotelydons and roots (c-h), mature plant (i), trichomes (i), hydathodes (indicated by arrows) (c-e, i), silique (o) and flower (n), including style, filament, receptacle and pedicel. No staining was detected in guard cells (m)

**No change in root system architecture in *plc7* and *plc5/7* mutants**

Knock-out/down mutants of *PLC3* or *PLC5* were affected in their primary- and lateral root growth formation. However, a double *plc3/5* mutant did not reveal a stronger effect, indicating that there might be a third *PLC* involved. (Zhang et al., 2017; Chapters 2, 3). To investigate the role of *PLC7* we identified two homozygous T-DNA insertion lines, *plc7-3* (SALK_030333) and *plc7-4* (SALK_148821) (Fig. 2a). Reduction of *PLC7* expression in *plc7-3* and *plc7-4* mutants was confirmed by Q-PCR (Fig. 2b) and revealed that the former is a KO- and the latter a KD mutant. However, the root architecture of 12 days old seedlings of these *plc7* mutants did not differ from the wild-type (Fig. 2c, d).

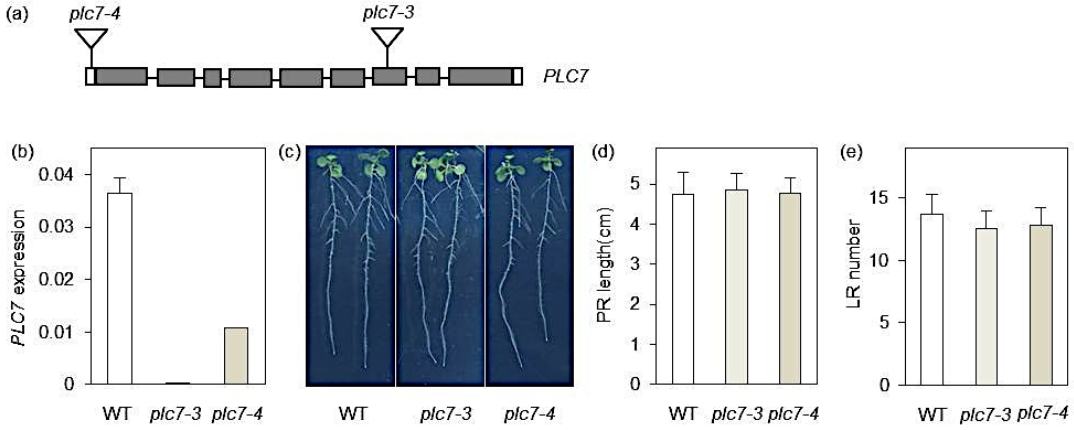


**Figure 2.** In contrast to *plc3*- and *plc5* mutants, KO- or KD mutants of *PLC7* are not affected in root development.
(a) T-DNA insertion positions (triangles) in the *PLC7* gene of *plc7-3* and *plc7-4* lines. Filled boxes and lines represent exons and introns, respectively, while open boxes represent untranslated regions. (b) *PLC7* expression levels in wild-type, *plc7-3* and *plc7-4* measured by Q-PCR using *SAND* as a reference gene. Values are the means ± SD (n = 3) of a representative experiment that was independently repeated at least three times. (c) Seedling morphology of wild-type, *plc7* mutants. Seeds were first germinated on ½MS with 0.5% sucrose for 4 days and then transferred to ½MS plates without sucrose. Photographs were taken 12 days after germination (DAG). (d) Primary root (PR) length and (e) lateral root (LR) number at 12 DAG. Values are means ± SE of three independent experiments (n>20). Asterisk (*) indicate significance at P<0.05 compared to wild-type, based on Student's *t* test.

To analyze gene redundancy, we tried to generate *plc3/5/7*-triple mutants by crossing *plc7-3* with the *plc3/5*-double mutant. However, the *plc3/7* combination turned out to be lethal and only homozygous *plc5/7*-double mutants could be obtained (Fig. 3a). As shown in Figures 3b-d, no significant difference was found between the root system of *plc5/7*- and wild-type seedlings.

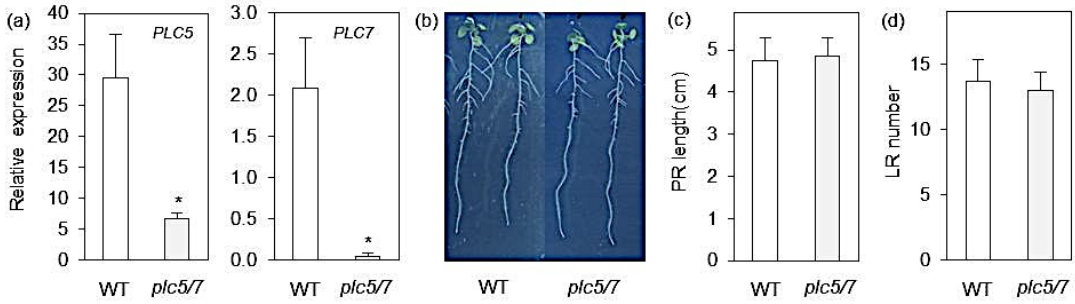


**Figure 3.** A *plc5/plc7* double mutant is viable and is not affected in root architecture.
(a) *PLC5* (left) and *PLC7* (right) expression in wild-type and *plc5/7*-double mutant. Relative expression is based on the expression of *SAND* measured by Q-PCR. Values are means ± SD (n = 3) of a representative experiment that was repeated at least three times. (b) Seedling morphology of wild-type and *plc5/7*. Seeds were germinated on ½MS with 0.5% sucrose for 4 days and then transferred to ½MS plates without sucrose. Photographs were taken 12 days after germination (DAG). (c) Primary root (PR) length and (d) lateral root (LR) number at 12 DAG. Values are means ± SE of three independent experiments (n>20). Asterisk (*) indicate significance at P<0.05 compared to wild-type, based on Student's *t* test.

### *plc5/7* mutant displays loose seed coat mucilage and reduced cellulose rays

While imbibing seeds for stratification, we noticed that the volume of the seed pellet of *plc5/7* seeds was always smaller than wild type after overnight incubation (Fig. 4a). Upon imbibition, the seed coat-epidermal cells normally extrude a mucilage that forms two transparent layers (adherent and non-

adherent layers) around the seed. To examine whether the smaller volume of the *plc5/7* mutant was caused by a mucilage defect, we stained imbibed seeds with Ruthenium red (Fig. 4b), which stains pectins, the main component of mucilage (Western *et al.*, 2000; Macquet *et al.*, 2007). Compared to wild-type, the adherent and non-adherent layers were more expanded in the *plc5/7* mutant (Fig. 4b, top panel) and when seeds were mildly shaken to remove the non-adherent layer, or treated with EDTA, *plc5/7* seeds lost the adherent layer completely(Fig. 4b, middle and lower panel, respectively).

Increased solubility of the pectins has been linked to perturbation of cellulose deposition (Harpaz-Saad *et al.*, 2011; Mendu *et al.*, 2011; Sullivan *et al.*, 2011; Yu *et al.*, 2014; Ben-Tov *et al.*, 2015; Basu *et al.*, 2016; Hu, Li, Wang, *et al.*, 2016; Hu, Li, Yang, *et al.*, 2016). To test this, wild-type and *plc5/7* seeds were stained with Calcofluor White (CFW, for cellulose and other β-glucans staining; (Fig. 4c, left panel) and Pontamine S4B (cellulose-specific dye; (Fig. 4c, right panel) (Willats *et al.*, 2001; Anderson *et al.*, 2010; Wallace and Anderson, 2012). In wild-type seeds, the primary cell wall remnants, and rays extending from the columella were stained by both dyes (Fig. 4c). The *plc5/7* seeds showed a similar staining pattern, but the CFW intensity was lower and the rays were clearly reduced compared to wild-type. These results point to a role for *PLC5* and *PLC7* in cellulose ray formation, which is a completely novel function for PLC.

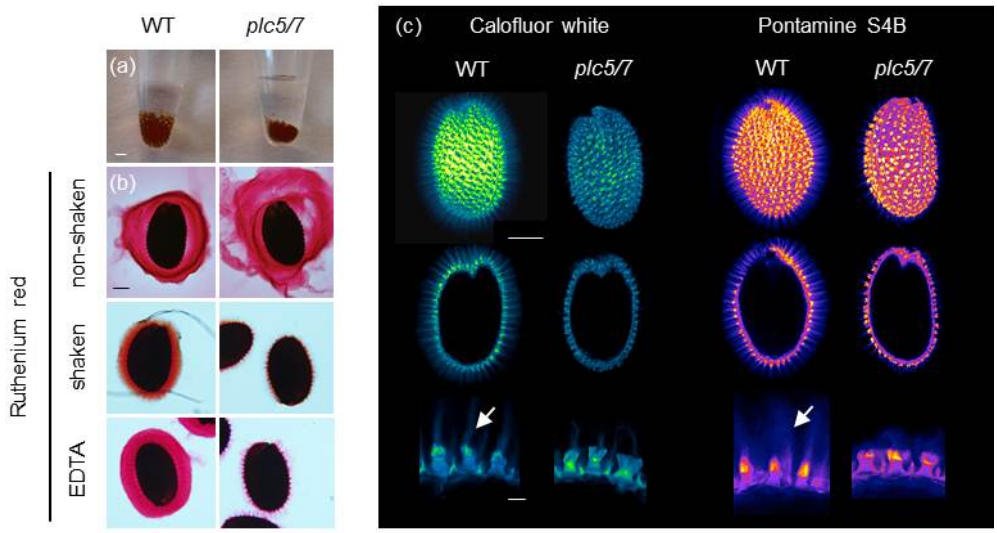


**Figure 4.** Seeds of *plc5/7* double mutant exhibit mucilage phenotype.
(a) Seeds of *plc5/7* swell less during imbibition. Equal amounts of dry seeds of wild type and mutant were immersed in water overnight and photographed the next day. (b) Ruthenium red staining of wild type- and *plc5/7* seeds, without shaking (top), with shaking (middle) and EDTA treatment. With shaking shows adherent mucilage layer; without shaking displays both adherent and non-adherent mucilage layers. (c) Cellulose staining by Calcofluor white (left panel) or Pontamine B (right panel) in wild type- and *plc5/7* seeds. Confocal images of whole seeds, cross section, and close-up views (top, middle and bottom, respectively) are shown. Bars represent 2 mm (a), 0.1mm (b), 0.1mm (top and middle rows) or 0.025 mm (bottom row) (c).

### *PLC5* and *PLC7* expression in developing seed

To further investigate the expression pattern of *PLC5* and *PLC7* during seed development, *pPLC5::GUS* and *pPLC7::GUS-SYFP* lines were used for additional histochemical analyzes (Fig. 5). At 4 day after pollination (DAP), some GUS activity was found in *pPLC5::GUS* (Fig. 5a, left panel)

while a strong staining in the seed coat and chalazal area of *pPLC7::GUS-SYFP* was observed (Fig. 5b). Later in development (at 8 and 10 DAP), GUS activity became stronger, with *PLC5* expression appearing in the seed coat and funiculus (Fig. 5a) and *PLC7* staining became stronger in seed coat and chalazal (Fig. 5b).

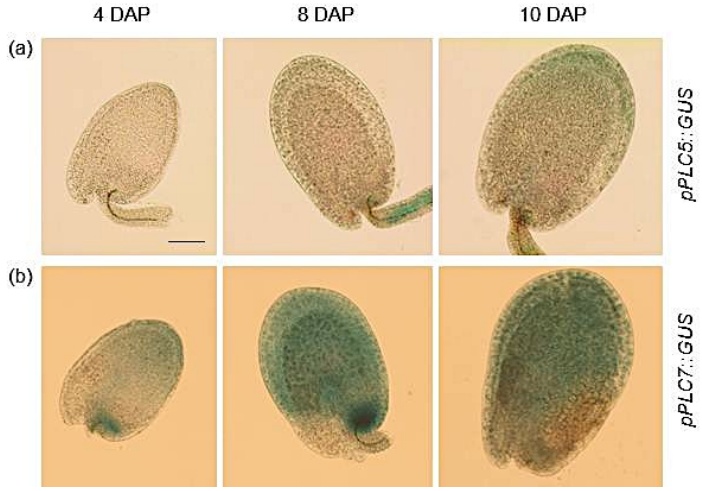


**Figure 5**. *PLC5* and *PLC7* expression during seed development.
(a) GUS activity analysis in *pPLC5::GUS* developing seeds. Expression was found in the funiculus at 8 days after pollination (DAP) and seed coat at 10 DAP. (b) GUS activity analysis in *pPLC7::GUS* developing seeds. Staining was found in the chalazal and in the seed coat. Bar = 0.1 mm

**Analysis of PPI- and PA levels in developing and germinating seeds**

To analyze the levels of the potential PLC substrates (i.e. PIP and $PIP_2$) and product (PA conversion of PLC-generated DAG), $^{32}P_i$-labelling (24h) of wild-type- and *plc5/7* mutant seeds at 10 DAP were compared with germinating, mature seeds. As shown in Figure 6, wild-type and *plc5/7* seeds were found to contain similar amounts of $PIP_2$, PIP and PA in both stages. Interestingly, PIP- and PA levels were much higher in developing seeds while $PIP_2$ levels were similar in both stages.

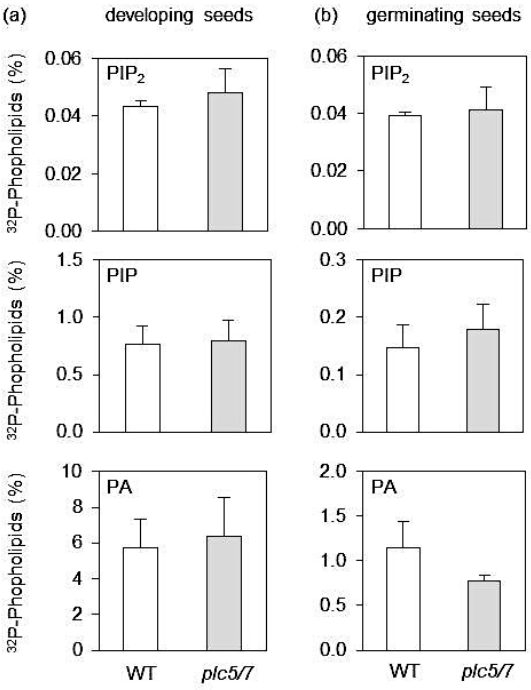


**Figure 6**. PPI- and PA levels in developing- and germinating (mature) seeds of wild type and *plc5/7*.

(a) Developing seeds, ~200 seeds at 10 DAP of wild type and *plc5/7* were labelled with $^{32}PO_4^{3-}$ for 24 h and their lipids extracted, separated by TLC and quantified by Phosphoimaging. (b) Mature seeds (~200) of wild type and *plc5/7* were pre-germinated on ½MS with 0.5% sucrose plates until testa ruptured, then labelled with $^{32}PO_4^{3-}$ for 24 h. Lipids were then extracted, separated and quantified as above. $^{32}$P-levels of $PIP_2$, PIP and PA are expressed as percentage of total $^{32}$P-phospholipids. Three independent experiments were performed; data shown are means ± SD (n=3) from one representative experiment.

**Leaves of *plc5/7* plants display enhanced level of leaf serration**

Growing *plc5/7* mutants on soil for longer periods of time revealed a novel phenotype in leaf-edge patterning (serration). Overall, the level of serration in successive rosette leaves was significantly increased in *plc5/7* mutant, which appeared to be stronger in the proximal part of the blade than in the distal part (Fig. 7a, b). To quantify this in more detail, we measured various parameters of the 8$^{th}$ leaf (Fig. 7c-e) of 4 -weeks old rosettes of both genotypes. No changes in blade length were observed between wild-type and *plc5/7*, but the blade width, -perimeter and -area were slightly, although not significantly, bigger in *plc5/7* (Fig 7d). The serration number was not changed in the *plc5/7* mutant, but the serration level (indicated by the ratio between the distance from midvein to tip and the distance from midvein to sinus, see Fig. 7c) was significantly higher in three successive teeth (Fig. 7f).

Recent studies have indicated that Arabidopsis leaf-margin development is controlled by a balance between *microRNA164A* (*MIR164A*) and *CUP-SHAPED COTYLEDON2 (CUC2)* (Nikovics *et al.*, 2006). Hence, we compared the expression of *MIR164A* and *CUC2* in wild-type and *plc5/7* leaves. As shown in Figure 7g, *plc5/7* leaves were consistently (3 independent experiments) found to contain higher levels of *CUC2* and lower levels of *MIR164A*, resulting in a significant increase in the *CUC2*/*MIR164A* ratio.

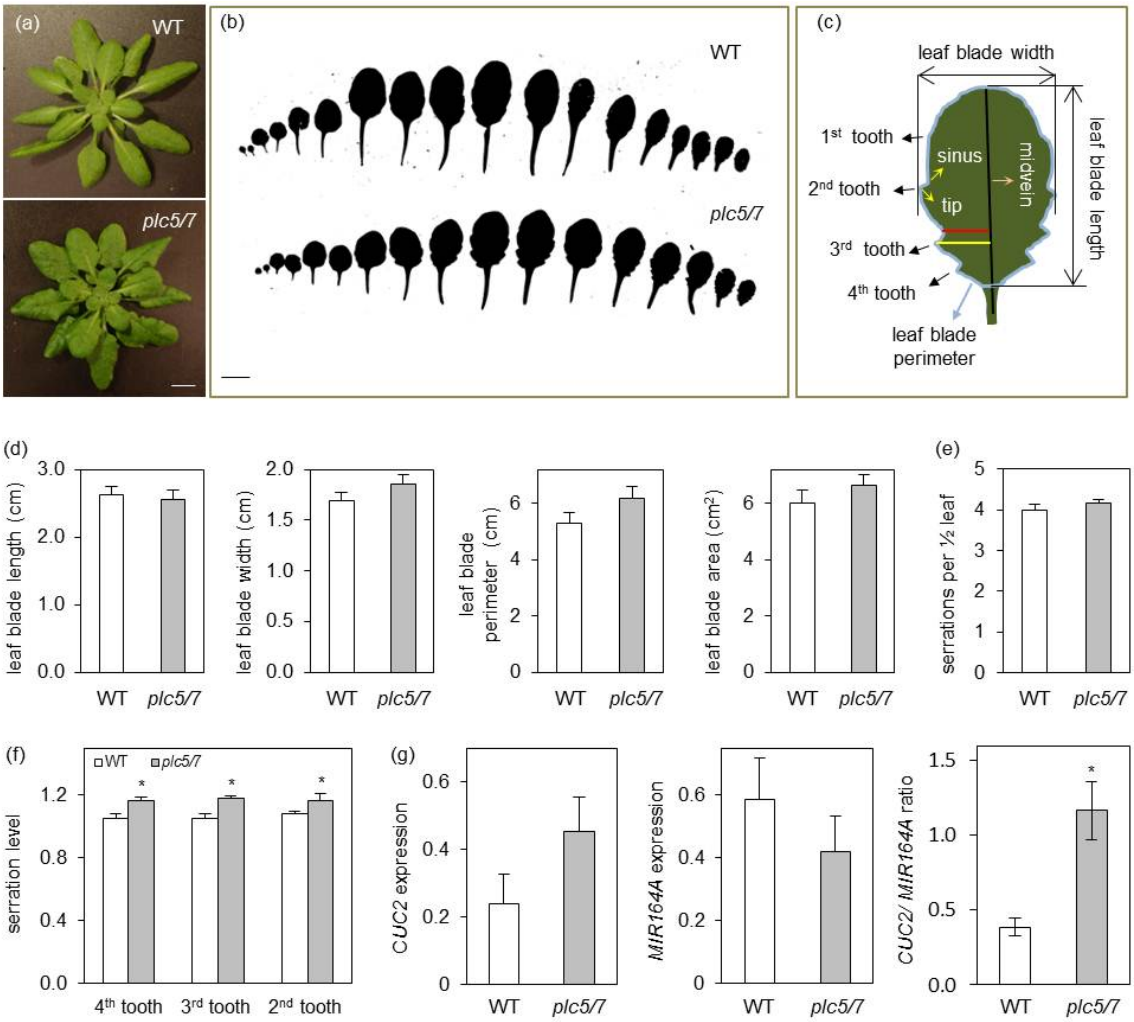


**Figure 7**. Leaves of *plc5/7* plants display enhanced leaf serration
(a) Phenotype of wild type- and *plc5/7* rosette. Rosettes of 4-week old plants grown in short day conditions, were cut and photographed immediately. Bar = 1 cm. (b) Leaf series of 4-week old wild type and *plc5/7* plant. (c) Cartoon to demonstrate the leaf parameters measured of the 8th leaf. (d) Quantification of blade size including, length, width, perimeter and area. (e,f) Quantification of leaf serration number (e) and level (f) in wild type and *plc5/7* mutant. (g) Expression of *CUC2* and *MIR164A* and their ratio in wild type and *plc5/7* mutant. Expression is relative to the expression of *OTC*. Three independent experiments were performed. Data in (g) represents the means ± SD (n=3) from one representative experiment that was repeated twice with similar results. Asterisk (*) indicate significance at P<0.05 compared to wt, based on Student's *t* test.

### The *plc5/7* mutant displays enhanced tolerance to drought

When plants were left in the greenhouse without watering, we noticed that *plc5/7* mutants appeared to be more drought tolerant while the single mutants behave like wt (data not shown). Performing multiple drought tolerance assays indeed confirmed this (Fig. 8a), and detached rosettes of 4-week-old *plc5/7* plants were found to loose less water than wild-type (Fig. 8b).

ABA plays a key role during the response to dehydration stress and is known to induce stomatal closure to reduce the loss of water (Sean *et al.*, 2010). Hence, we checked the stomatal-closure of *plc5/7* and wild-type in response to ABA. As shown in Figure 8c, *plc5/7* has less-opened stomata compared to

wild-type without ABA, but when ABA was applied, stomata closed in genotypes, although the *plc5/7* mutant appeared to be less responsive.

Previously, we found that overexpression of *PLC3* or *PLC5* enhanced drought tolerance in Arabidopsis (Zhang et al., 2017; Chapters 2, 3), which was earlier also revealed for maize, canola and tobacco (Wang *et al.*, 2008; Georges *et al.*, 2009; Tripathy *et al.*, 2011). We therefore wondered whether the increase in drought tolerance in *plc5/7* was a result of the overexpression of any of the other (redundant) 7 *PLCs*. However, no strong overexpression of any *PLC* was found in *plc5/7* (Fig. 8d). In fact, *PLC1*, *PLC2* and *PLC4* were found to be slightly down-regulated (Fig. 8d).

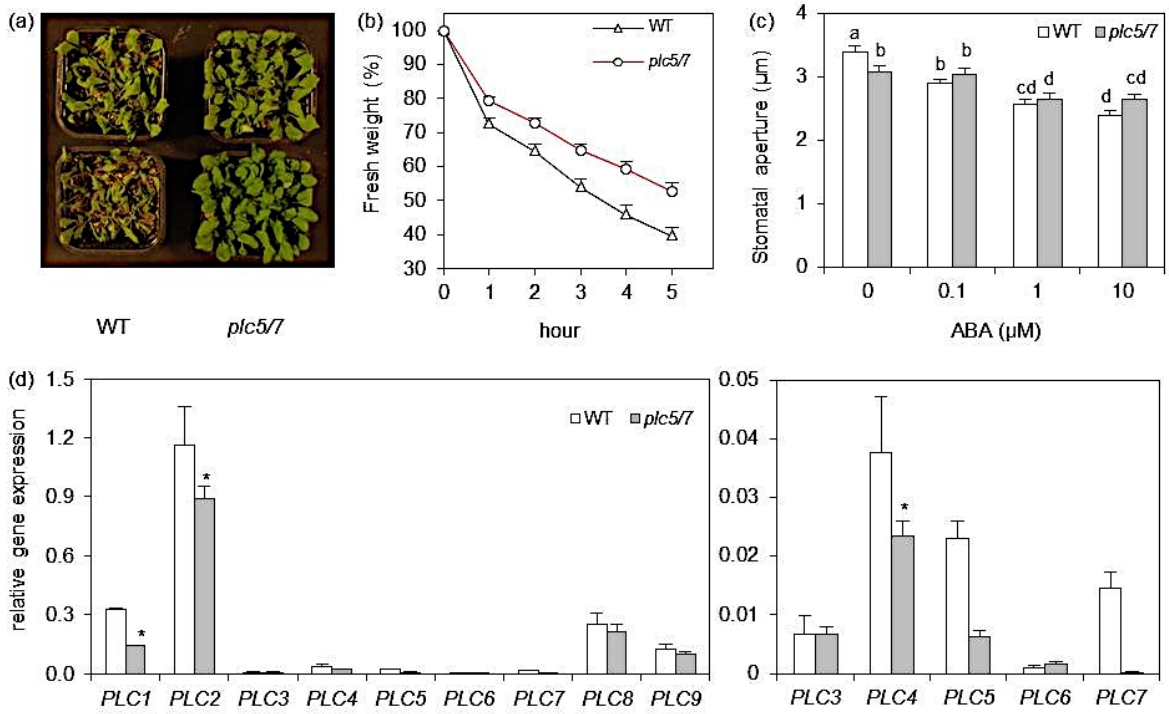


**Figure 8**. Soil-grown *plc5/7* mutant are more tolerant to drought stress.
(a) Six-weeks old plants of wild type- or *plc5/7* mutant plants, grown on soil and exposed to drought by withholding water for the last two weeks and then were photographed. (b) Water loss of detached rosette of normally watered, 4-weeks old plants. Water loss was measured at indicated time points and expressed as a percentage of the initial fresh weight. Values are means ± SD for one representative experiment (n=36). (c) Effect of ABA on the stomatal aperture in leaf strips of wild type and *plc5/7* plants. Leaves from 3-weeks old plants were stripped and the peels were incubated in opening buffer with light for 3 h until stomata were fully open. Peels were then treated with different concentrations of ABA for 90 mins, after which stomata were digitized and aperture widths measured. Values are means ± SE of at least three independent experiments (n >100). Data was analyzed by 2-way ANOVA. Statistical significant differences between genotypes are indicated by letters ($P<0.05$, Dunn's method). (d) *PLC1- PLC9* expression level in wild type and *plc5/7* mutant plants as measured by QPCR, relative to the amount of *SAND*. Values are means ± SD (n = 3) for one representative experiment that was repeated two times with similar results.

### *Overexpression of PLC7* increases drought tolerance

As mentioned above, overexpression of Arabidopsis *PLC3* and *PLC5*, which are from different subfamilies than *PLC7*, resulted in enhanced drought tolerance (Zhang et al., 2017; Chapters 2 and 3). To check the effect of *PLC7* overexpression, homozygous T3 plants were generated. Two lines, *PLC7-OE9* and *PLC7-OE12*, which overexpressed *PLC7* around 80- to 100-fold, respectively, were selected for further studies, (Fig. 9a). Both lines were indeed found to be more drought tolerant than wild-type (Fig. 9b), and lost slightly less water when rosettes of 4-week-old plants were detached (Fig. 9c). The stomatal aperture and their response to ABA was found to be similar to wild-type (Fig. 9d), which is different to *PLC3-* and *PLC5-OE* plants that had stomata that opened less wide than the wt.

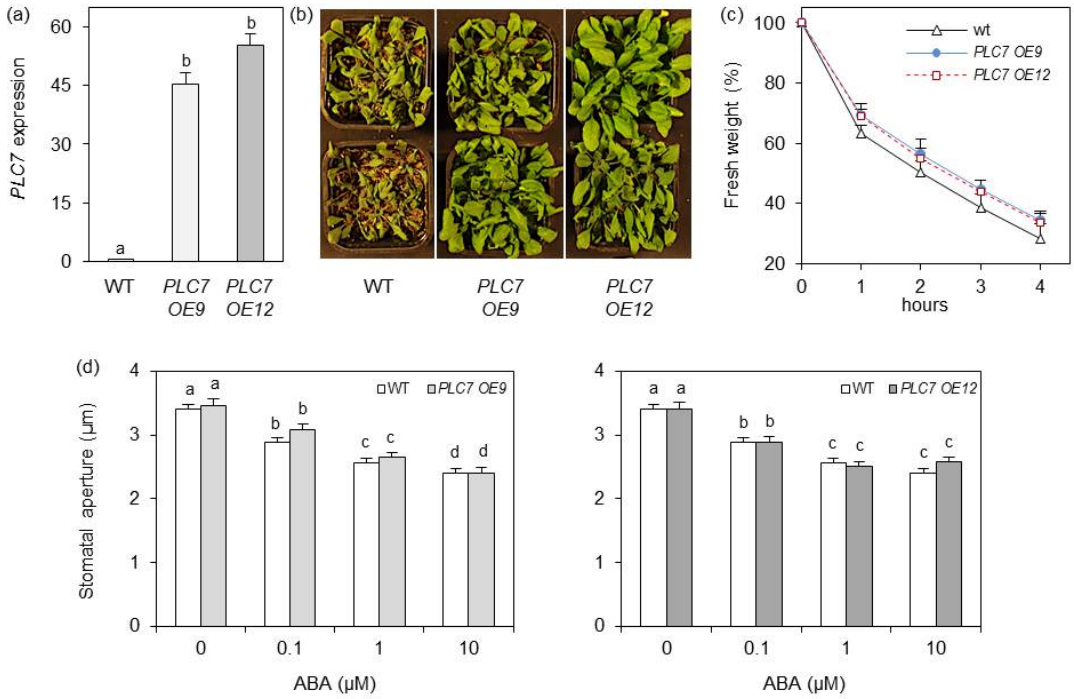


**Figure 9.** Overexpression of *PLC7* enhances drought tolerance.
(a) *PLC7* expression levels in wild type and two homozygous *PLC7* overexpression lines, *PLC7-OE9* and *PLC7-OE12* as measured by Q-PCR and based on the expression of the *SAND* reference gene. Values are means ± SD (n = 3) for one representative experiment. (b) Phenotype of six week old plants from wild type and *PLC7*-overexpresion lines, *#OE9* and *#OE12*, after two weeks of drought stress. (c) Water loss of detached rosette of four weeks old plants. Water loss was measured at indicated time points and expressed as a percentage of the initial fresh weight. Values are means ± SD for one representative experiment (n=36). (d) Stomatal aperture in leaf peels of wild type, *PLC7-OE9* (left), *PLC7-OE12* (right) and the effect of ABA. Leaves from 3-weeks old plants were stripped and peels were incubated in opening buffer with light for 3 h until stomata were fully open. Peels were then treated with different concentrations of ABA for 90 mins, after which stomata were digitized and the aperture width measured. Values are means ± SE of at least three independents (n > 100). Data was analyzed by 2-way ANOVA. Statistical significant differences between genotypes are indicated by letters (P<0.05, Dunn's method).

**Phospholipid responses upon osmotic stress**

To analyze the phospholipid responses in *plc5/7* and the *PLC-OE* lines, $^{32}$P-labeling experiments (3 hrs labeling) were performed on seedlings, and the effect of sorbitol treatment was tested to mimic osmotic stress. Both *plc5/7* and wild-type showed similar levels of PPI- and PA in absence of sorbitol (Figs. 10a, b). Upon sorbitol treatment, a stronger $PIP_2$ response was typically observed in the *plc5/7* lines though numbers appear not to be statistically different. While $PIP_2$ levels increased by ~4 times in wild-type, *plc5/7* seedlings typically exhibited a 6-times increase. No difference in PA- or PIP response was observed (Fig. 10b).

*PLC7-OE* lines revealed no difference in PPI or PA levels compared to wild-type in control conditions (Fig. 10c, d). However, with sorbitol, again a stronger $PIP_2$ response was observed in *PLC7-OE* lines, ~6-times *vs* ~4-times for wild-type, while PA- and PIP responses were similar (Fig. 10c, d). These results suggest that both *plc5/7* and *PLC7-OE* plants boost more $PIP_2$ in response to osmotic stress than wild-type, similar to what we found earlier for *PLC3-* and *PLC5-OE* lines (Chapters 2, 3).

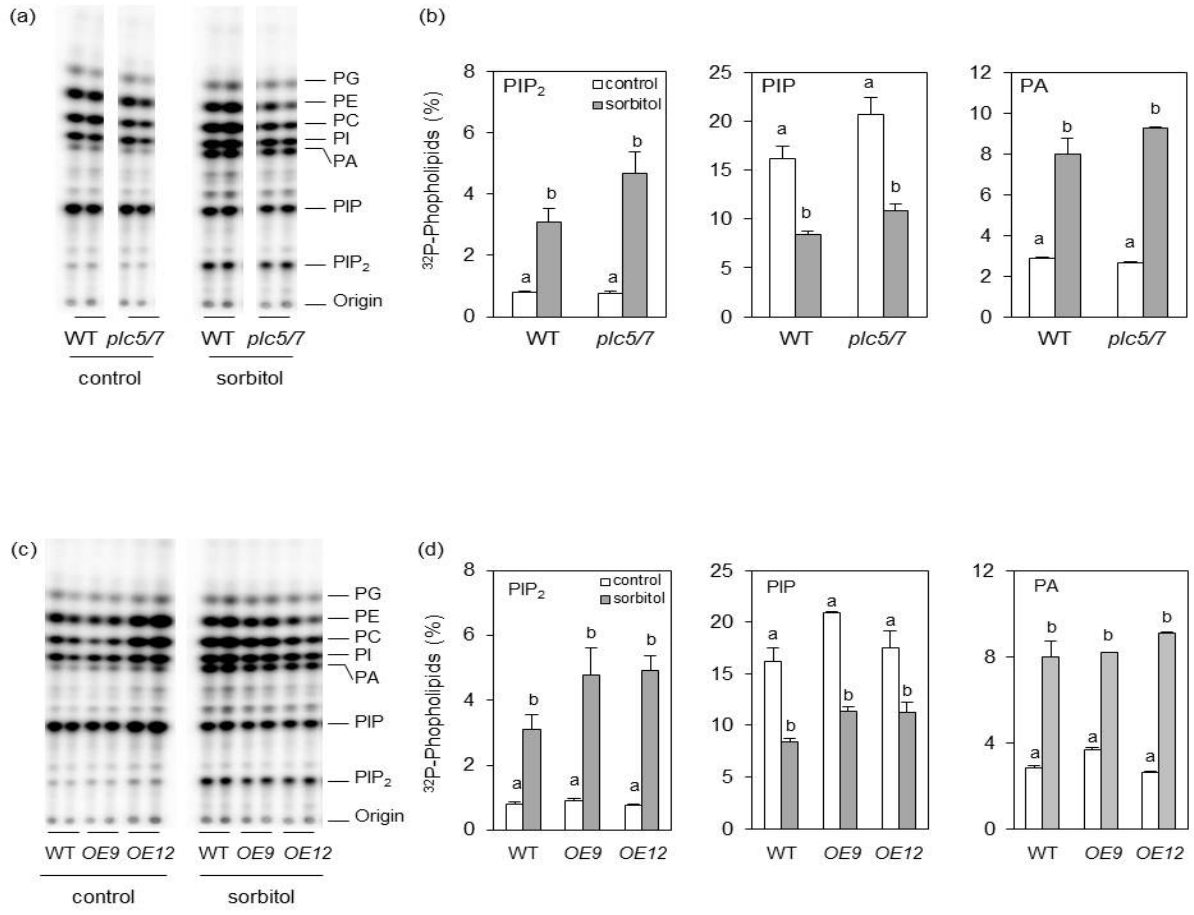


**Figure 10.** Both *plc5/7* and *PLC7* over-expressers displayed stronger $PIP_2$ response upon osmotic stress.
Six-day-old seedlings were $^{32}$P-labeled for 3h and then treated with buffer ± 600 mM sorbitol for another 30 min. Extracted lipids were analyzed by TLC and quantified through phosphoimaging. (a and c). Typical TLC profile with each lane representing the extract of 3 seedlings. (b, d) $^{32}$P-levels of $PIP_2$, PIP and PA of wild-type and *plc5/7* (b) or *PLC7-OEs* (line #9 and #16) (d) with and without sorbitol. Three independent experiments were performed. Data shown are the means ± SE (n=3) from three independent experiments. Data was analyzed by 2-way ANOVA. Statistical significant differences between normal and sorbitol conditions in wild type and *plc5/7* or *PLC7-OEs* are indicated by letters ($P<0.05$).

## DISCUSSION

### Knockout of *PLC7* does not affect root architecture

Previously, we demonstrated that Arabidopsis *PLC3* and *PLC5* were both involved in lateral root formation and that a *plc3/5*-double mutant did not exhibit a more severe phenotype than single mutants (Chapters 2, 3). We therefore speculated that another PLC must be involved. Since promotor-GUS analyses revealed specific expression in phloem companion cells and a typical segmented pattern in the vascular of the primary root from which lateral roots emerged, we specifically searched for other phloem-specific PLCs. Using the eFP browser, we found two potential candidates, *PLC2* and *PLC7*. Since T-DNA insertion mutants of *PLC2* were lethal (D'Ambrosio *et al.*, 2017; Di Fino *et al.*, 2017; R. van Wijk and Munnik, unpublished), we focused on *PLC7*. Two independent homozygous T-DNA insertion mutants were obtained, with *plc7-3* being a KO- and *plc7-4* a KD line. Both mutants exhibited normal root architecture. In an attempt to create double- and triple mutants of the redundant *PLCs*, we crossed the *plc3-2/plc5-1* (*plc3/5*; Chapter 3) with *plc7-3*, but this only resulted in viable *plc5/7* double mutants, as the combination *plc3/plc7* turned out to be lethal (not shown). The *plc5/7* double mutant, however, did not reveal any significant changes in root morphology (Figs. 2, 3). While *pPLC7-GUS* analyses confirmed the vascular expression of *PLC7*, the typical segmented pattern found for *PLC3* and *PLC5* was not found. These results may indicate that *PLC2* is the redundant *PLC* in root development, and preliminary results from this laboratory, using induced silencing (R. van Wijk and T. Munnik, Unpublished), confirm this. Interestingly, *PLC7* was also expressed in hydathodes and in seeds, which correlates well with the two new phenotypes that were found for *plc5/7*-double mutants, which have never been observed before. These include a mucilage phenotype in seeds and a serration phenotype in leaves. The latter may correlate with *PLC7*'s expression at hydathodes. *PLC7* was also strongly expressed in trichomes. *PLC5* is also expressed there, although less, and *PLC3* is typically expressed only in the trichome basal cells of developing leaves (Chapters 2, 3). We checked for trichome phenotypes in individual *plc3, plc5 or plc7* and *plc3/5*- and *plc5/7*- mutants, but found no obvious effect (number, shape) was visible. Again, this could be due to redundancy, or PLC is involved in content of, or transport to the trichomes, which would not lead to an obvious phenotype.

Strikingly, and new to PLC loss-of-function lines, is that *plc5/7* mutants were more drought tolerant, a phenotype that is typically found when *PLC* is overexpressed (Chapter 2 and 3; Wang *et al.*, 2008; Georges *et al.*, 2009; Tripathy *et al.*, 2011). However, we found no upregulation of redundant PLCs in the *plc5/7*-mutant background. If anything, some down regulation of *PLC1*, *PLC2* and *PLC4*. RNASeq analyses of the *plc* mutant and OE lines may shed light on potential pathways that are up- or down-regulated to explain various phenotypes. Most importantly, altering expression of *PLC* genes results in clear phenotypes and this will further help elucidating the role of PLC in plant signaling and development.

While several new pieces of the PLC-signaling puzzle (new phenotypes) in plants have been found, it remains unclear how this is achieved at the cellular and molecular level. It is clear that plants lack the prime targets for $IP_3$ and DAG, and there are several indications that responses are coupled via inositolpolyphosphates (IPPs) and/or PA (Wang *et al.*, 2006; Arisz *et al.*, 2009, 2013; Munnik and Vermeer, 2010; Munnik and Nielsen, 2011; Testerink and Munnik, 2011; Gillaspy, 2013; Munnik, 2014; Laha *et al.*, 2015; Heilmann, 2016; Hou *et al.*, 2016). Alternatively, since PIP or $PIP_2$ are emerging as second messengers themselves, PLC could function as an attenuator of signaling too. In that respect, it is interesting to notice that the increased drought-tolerant phenotype in *plc5/7* and the *PLC3*, *-5*, and *-7* overexpression lines correlates with a stronger $PIP_2$ response in seedlings osmotically stressed with sorbitol. How this would work remains unclear, but these lines could somehow be primed for an enhanced $PIP_2$ turnover.

**Role for *PLC5* and *PLC7* in seed mucilage**

Mucilage is a complex of polysaccharides, which is from seed coat epidermal cells when seeds are exposed to an aqueous environment(Western *et al.*, 2000). The major component of mucilage is pectin, of which polygalacturonic acid (PGA) and rhamnogalacturonan I (RGI) are the most common compounds found in cell walls and mucilage (Carpita and Gibeaut, 1993; Cosgrove, 1997). In addition to pectin, mucilage also contains some minor monosaccharides, i.e. arabinose, galactose, glucose, xylose and mannose, which are equally important in controlling mucilage properties(Voiniciuc, *et al.*, 2015). The extruded mucilage contains two layers, a non-adherent outer layer and an adherent inner layer. The former is easily removed from the seed (Harpaz-Saad *et al.*, 2011; Mendu *et al.*, 2011; Sullivan *et al.*, 2011). The latter is hard to detach, even chemically (Macquet *et al.*, 2007). Our result showed that inner mucilage of *plc5/7* seed coats was easily lost (Fig. 4b). Many factors are involved in maintaining the adherence of the inner mucilage, with cellulose being the most important (Harpaz-Saad *et al.*, 2011; Sullivan *et al.*, 2011; Yu *et al.*, 2014; Ben-Tov *et al.*, 2015; Voiniciuc, Schmidt, *et al.*, 2015; Hu, Li, Wang, *et al.*, 2016; Hu, Li, Yang, *et al.*, 2016). Staining with Calcofluor white and Pontamin S4B indicated that certain cellulose rays were missing from *plc5/7* seed-coat mucilage (Fig. 4c). We checked for sugar-composition aberrations in whole seeds, but found no changes compared to wild-type (Supplemental Fig. S1). Possibly, the distribution between non-adherent and adherent mucilage layers might be different, which needs to be further determined. The adherence of mucilage by cellulose is mainly caused by its crystallization by self-association via hydrogen bonding (Sullivan *et al.*, 2011), and several genes have been recently reported to regulate cellulose crystallization, i.e. *COBRA-LIKE2*, *IRX14* and *IRX7* etc (Ben-Tov *et al.*, 2015; Hu, Li, Wang, *et al.*, 2016; Hu, Li, Yang, *et al.*, 2016).

Histochemical analysis of the GUS reporter lines indicated that both *PLC5* and *PLC7* are expressed during seed development (Fig. 5). Until now, no mucilage deficiency has been linked to *PLC*, and we only observed the mucilage phenotype in the *plc5/7*-double mutant of all our *PLC* knockout

mutants. The defect in both *PLC5* and *PLC7* probably breaks the balance for mucilage maintenance by altering cellulose deposition and/or crystallization in the inner mucilage. How the enzyme PLC could be involved in all this will require additional research. Potentially, PLC could be required for mucilage secretion or for the localization or activity of cellulose synthases, for example. PA, PIP and $PIP_2$ have been implicated to play essential roles in vesicular trafficking, -fusion and -fission. Even though no difference was found in PPI- or PA levels in either developing or mature seeds (Fig. 6), reduced amounts of PLC5 and lack of PLC7 might cause crucial local changes in lipid or IPP molecules.

**Role for *PLC* in leaf serration**

Leaf shape is defined by the pattern and degree of indentation at the margin area, thus distinguishing plant species (Tsukaya, 2006). The patterning involves a complex crosstalk between hormone signaling and genetic regulators (Byrne, 2005; Fleming, 2005). Leaf serration is an important patterning event and its development involves auxin maxima at the protrusion of each serrated section (Hay and Tsiantis, 2006). Based on recent genetic studies, the auxin efflux carrier PIN-FORMED 1 (PIN1) and CUP-SHAPED COTYLEDON 2 (CUC2) have been identified as two key factors required for the formation of leaf serration (Hay *et al.*, 2006; Nikovics *et al.*, 2006). PIN1 asymmetrically localizes on plasma membranes and directionally transports auxin, creating auxin maxima that direct the outgrowth of the serrations (Hay *et al.*, 2006; Scarpella *et al.*, 2006). CUC2 is a transcription factor that is post-transcriptionally downregulated in leaves by *MIR164A* (Nikovics *et al.*, 2006). CUC2 expression is limited to the sinus where the serration starts, and the promotion of serration outgrowth is through cell division, not by suppression of sinus growth (Kawamura *et al.*, 2010). CUC2 has also been indicated to regulate the polarized localization of PIN1 in convergence points at the leaf margin, playing a role in establishing, maintaining and/or enhancing auxin maxima that result in leaf serration (Kawamura *et al.*, 2010; Bilsborough *et al.*, 2011). In a feedback loop, auxin downregulates *CUC2*, both transcriptionally and post-transcriptionally through activation of *MIR164A* (Bilsborough et al., 2011).

The *plc5/7*-double mutant revealed a mildly-enhanced leaf-serration phenotype (Fig. 7) Subsequent measurement of *CUC2* and *MIR164A* expression revealed a an up-regulation of *CUC2* and down-regulation *MIR164A*, which is consistent with the enhanced serration (Kawamura *et al.*, 2010; Bilsborough *et al.*, 2011). Promotor-GUS analyses showed that both *PLC5* and *PLC7* were expressed at leaf hydathodes, a secretory tissue that secretes water through the leaf margin that is also associated with leaf serration (Tsukaya and Uchimiya, 1997) and auxin response maxima (Scarpella *et al.*, 2006). Hence, it is possible that *PLC5* and *PLC7* together contribute to the regulation of leaf serration, also because there was no such phenotype found in single mutants. We also measured PPI-and PA levels in *plc5/7* rosette leaves but, like seeds and seedlings, found no changes (data not shown; Figs. 6 and 10). It is possible that differences are limited to particular cells or tissues and that most of the cells have normal levels/responses. How *PLC5* and *PLC7* are involved in leaf serration requires further investigation. $IP_6$ could play a positive role in auxin signaling through activation of TIR1 (Chapter 2).

However, increased leaf serration would then be expected to result from increased $IP_6$ formation, which not what we would directly expect from a *plc5/7* mutant. On the other hand, $PIP_2$ has been suggested to play a role in the polarized localization of PIN1(Ischebeck *et al.*, 2013; Tejos *et al.*, 2014), in which PLC could also play a role. As mentioned earlier, down-regulation of these two PLCs (*plc5* KO is likely lethal; Chapter 3) could result in a local upregulation of another PLC, even though overall *PLC* expression levels (Fig. 8d) do not confirm such a model.

**Both *PLC7* overexpression and *plc5/7* down-regulation enhance drought tolerance**

Overexpression of *PLC* in maize, tobacco and canola improved drought tolerance (Wang *et al.*, 2008; Georges *et al.*, 2009; Tripathy *et al.*, 2011). Similarly, we found that overexpression of *PLC3* or *PLC5* increased the drought tolerance of Arabidopsis. To investigate the effect of *PLC7* overexpression, homozygous *pUBQ10::PLC7* lines were generated. Meanwhile, we took *plc5-1*, *plc7-3* and *plc5/7*-double mutants along to see how they would behave under drought stress. While plants appeared normal under control conditions, except for *plc5/7* showing more serrated leaves, upon drought stress both *plc5/7*- and *PLC7-OE* lines performed better (Figs. 8a, 9b), and lost less water than wild type (Figs. 8b, 9c), even though the latter was not statistically significant for *PLC7-OE* lines (Fig. 9c).

ABA synthesis is stimulated by dehydration stress and known to induce stomatal closure to reduce the water loss (Sean *et al.*, 2010). Previous result indicated that *PLC3*- and *PLC5-OE* lines showed a 'less-open stomata' phenotype in the absence of ABA, and that they exhibited a reduced closing response to ABA compared to wild-type (Chapters 2 and 3). Overexpression of *PLC7* did not show 'less-open stomata' under control conditions, and their response to ABA was like wild type. Stomata of *plc5/7* plants were less open but their response to ABA appeared normal, maybe slightly decreased, which is in contrast to *plc5*- and *plc7*-single mutants, which have a normal opening at control conditions, and *plc7* is less sensitive to ABA (Supplemental Fig. S2; Chapter 3). Interestingly, *PLC7* itself was not expressed in guard cells (Fig. 1), but the gene is rapidly upregulated in guard cells upon ABA treatment (Bauer *et al.*, 2013). Hence, it could be that the drought tolerant phenotype in the *plc5/7* is a consequence of a local upregulation (for instance in the guard cells) of one or more redundant *PLCs*, which may remain undetectable when whole seedling levels are measured (Fig. 9).

Osmotic stress-induced phospholipid signaling responses have been reported in many studies (Munnik and Vermeer, 2010; Meijer *et al.*, 2017). We measured PPI- and PA levels in response to sorbitol to mimic drought stress in *plc5/7*, *PLC7-OE* and wild-type seedlings using $^{32}P$-labeling. Under control conditions, no difference in PPI- and PA levels were found among the genotypes (Fig. 10). However, in response to osmotic stress, the $PIP_2$ response in both *plc5/7* and *PLC7-OE* lines were stronger than wild-type (Fig. 10b and 10d). Apart from second messenger precursor, $PIP_2$ could also play a role as signaling molecule itself, for example in the reorganization of the cytoskeleton, in endo- and exocytosis, or ion channel regulation (Stevenson *et al.*, 2000; Martin, 2001; van Leeuwen *et al.*, 2007; Heilmann, 2016). Identification and characterization of some of $PIP_2$'s main targets will be

essential to start unraveling the molecular mechanisms involved. Whether the above response in *plc5/7* is a consequence of enhanced, local expression of another *PLC*, or a consequence of differential gene expression and hence drought tolerant response, requires further studies.

## MATERIALS AND METHODS

### Plant material

*Arabidopsis thaliana* (*Col-0*) was used throughout. T-DNA insertion mutants *plc7-3* (SALK_030333) and *plc7-4* (SALK_148821) were obtained from the SALK collection (signal.salk.edu). Homozygous plants were identified by PCR in F2 generation using gene-specific primers. For the identification of *plc7-3*, we used forward primer 5'- GATTTGGGTGATAAAGAAGTTTGG -3'; reverse primer 5'- CTCCACACAATCTCAGCATTAC-3') and left border primer LBb1.3 (5'- ATTTTGCCGATTTCGGAAC-3', in combination with the forward primer). For *plc7-4* identification, forward primer 5'- TCCTTCCTGTTATCCATGACG -3'; reverse primer 5'- TTGAAGAAAGCATCAAGGTGG -3') and left border primer LBb1.3 (5'- ATTTTGCCGATTTCGGAAC-3', in combination with the reverse primer) were used. To generate double mutant *plc5/7*, *plc5-1* and *plc7-3* were used for crossing.

### Root growth

Seeds were surface sterilized in a desiccator using 20 ml thin bleach and 1ml 37% HCl for 3 hours, and then sowed on square petri dishes containing 30 ml of ½ strength of Murashige and Skoog (½MS) medium (pH 5.8), 0.5% sucrose, and 1.2 % Daishin agar (Duchefa Biochemie). Plates were stratified at 4 °C in the dark for two days, and then transferred to long day conditions (22 °C, 16 h of light and 8h of dark) in a vertical position, under an angle of 70°. Four-day-old seedlings of comparable size were then transferred to ½MS ager plates without sucrose and allowed to grow further for another 6-8 days. Plates were then scanned with an Epson Perfection V700 scanner and primary root length, lateral root number and average lateral root length from each genotype quantified through ImageJ software (National Institutes of Health).

**Cloning and plant transformation**

To generate *pPLC7::GUS-SYFP* reporter line, the *PLC7* promoter was amplified from genomic DNA using the following primers: PLC7proH3fw (5'-CCCAAGCTTGATCCTATCAATATTCCTAATTCAGC-3') and PLC7proNheIrev (5'-CTAGCTAGCTTGAACAATTCCTCAAGTG-3'). The PCR product was cloned into pGEM-T easy and sequenced. A *HindIII-pPLC7-NheI* fragment was then ligated into pJV-GUS-SYFP, cut with *Hind*III and *Nhe*I. A *pPLC7::GUS-SYFP1* fragment, cut with *Not*I and transferred to pGreenII-0229.

The MultiSite Gateway Three-Fragment Vector Construction Kit (www.lifetechnologies.com) was used to generate *PLC7* overexpression lines driven by the *UBQ10* promotor (*pUBQ10::PLC7*). Oligonucleotide primers (5'-GGGGACAACGTTTGTACAAAAAAGCAGGCTATGTCGAAGCAAACATACAAAGT-3' and 5'-GGGGACCACTTTGTACAAGAAAGCTGGGTCACAAACTCCAACCGCACAAGAA-3') including attB1 and attB2 sites, were used to PCR from *PLC7* cDNA and was cloned into the donor vector (pDONR207) by using BP Clonase II enzyme mix to create entry clone BOX2. BOX1 was *pGEM-pUBQ10* entry clone containing attL4 and attR1 sites. BOX3 was pGEM-TNOS entry clone containing attR2 and attL2 sites. Both entry clone were obtained from university of Amsterdam plant physiology publish construct source. The three entry clones (BOX1, BOX2 and BOX3) and a destination vector (pGreen0125) were used in MultiSite Gateway LR recombination reaction to create the expression clone. For details, check: (Multi gateway protocol).

All constructs were transformed into *Agrobacterium tumefaciens,* strain GV3101, which was subsequently used to transform Arabidopsis plants by floral dip (Clough and Bent, 1998). Homozygous lines were selected in T3 generation and used for future experiments.

**RNA extraction and Q-PCR**

The primer pairs to check for *PLC1*- to *PLC9*-expression levels were obtained from Tasma *et al.* (2008). Similarly, identification of *CUC2*- and *MIR164A*-expression levels were performed as described by Bilsborough *et al.* (2011). Total RNA was extracted with Trizol reagent (Invitrogen, Carlsbad, CA) as described by Pieterse (1998). Total RNA (1.5 μg) from 10-day-old seedlings, or 4-week old rosette leaves, were converted to cDNA using oilgo-dT18 primers, dNTPs and SuperSccript III Reverse Transcriptase (Invitrogen), according to the manufacturer's instructions. Q-PCR was performed with ABI 7500 Real-Time PCR System (Applied Biosystem). The relative gene expression was determined by comparative threshold cycle value. Transcript levels were normalized by the level of *SAND* (At2g28390; forward primer: 5'-AACTCTATGCAGCATTTGATCCACT-3', reverse primer: 5'-TGAAGGGACAAAGGTTGTGTATGTT-3'), or OTC (At1g75330; forward primer: 5'-TGAAGGGACAAAGGTTGTGTATGTT-3', reverse primer: 5'-CGCAGACAAAGTGGAATGGA-3') (Bilsborough *et al.*, 2011; Han *et al.*, 2013). Three biological- and two technical replicates were performed to obtain the values for means and standard deviations (Han *et al.*, 2013).

**Histochemical analyses for GUS activity**

GUS staining was performed as described previously (Chapter 2; Zhang et al., 2017). Briefly, transgenic plants carrying *pPLC7::GUS-SYFP* were grown for indicated times, after which specific tissues were taken and incubated in an X-Gluc reaction solution containing 1mg/ml 5-bromo-4-chloro-3 indolyl-β-D-glucuronic acid (X-gluc), 50 mM phosphate buffer (pH 7.0), and 0.1% TX-100. Material was incubated overnight at 37°C and the next day, cleared by 70% ethanol, and kept in that solution. GUS staining was visualized under a stereo microscope (Leica MZFLIII) and digitalized with a ThorLabs, CCD camera.

**Seed staining and microscopy**

To visualize seed coat mucilage, mature dry seeds were stained as described in Macquet et al. (2007). Seeds were directly incubated in 0.03% (w/v) Ruthenium red, or after imbibition in 0.5 M EDTA, pH 8.0, for 90 min. For the latter, seeds were washed with water to remove the EDTA and then stained for 20 min with Ruthenium red. Stained seeds were routinely observed with a light microscope (Aristoplan; Leitz). To visualize the seed surface and the adherent mucilage (AM) layer by confocal microscopy, Calcofluor white (0.01%) and Pontamine S4B were used as staining solutions (Western *et al.*, 2000; Saez-Aguayo *et al.*, 2014). Optical sections were obtained with an Olympus LX81 spectral confocal laser-scanning microscope. A 405 nm diode laser line was used to excite Calcofluor white and the fluorescence emission was detected between 412 and 490 nm. For Pontamine S4B a 561 nm diode laser line was used and the detection was done between 570 and 650 nm. For comparisons of the signal intensity within one experiment, the laser gain values were fixed. Three different batches of seeds were analyzed and all of them showed the same phenotype. LUT green fire blue filter and LUT fire filter (Image J) were applied to the Calcofluor white and Pontamine S4B images, respectively.

## Determination of sugar composition by HPAEC-PAD

Sugar composition of wild-type and mutant seeds were measured as described previously (Saez-Aguayo *et al.*, 2017). 20 mg of seeds were ground in liquid nitrogen and extracted twice in 80% ethanol with agitation for 1 h at room temperature followed by removal of lipids by washing twice with methanol:chloroform (1:1) and twice with acetone. The final AIR was dried overnight at RT and two mg was hydrolyzed for 1 h with 450 µL 2 M trifluoroacetic acid (TFA) at 121 °C, using inositol as an internal control. TFA was evaporated at 60 °C with nitrogen, samples washed two times with 250 µL of 100% isopropanol, and dried in a speed-vac. Samples were dissolved in 200 µL Ultrapure water, clarified with a syringe filter (0.45 µm) and transferred to a new tube for analysis by High Performance Anion Exchange Chromatography with Pulsed Amperometric Detection (HPAEC-PAD).

The sugar quantification was done as described by Sáez-Aguayo et al. (2017). A Dionex ICS3000 ion-chromatography system, equipped with a PAD detector, a CarboPac PA1 (4mm x 250mm) analytical column, and a CarboPac PA1 (4mm x 50mm) guard column were used. The separation of neutral sugars was performed at 40ºC with a flow rate of 1 mL/min using an isocratic gradient of 20 mM NaOH for 20 min followed by a wash with 200 mM NaOH for 10 min. After every run, the column was re-equilibrated in 20 mM NaOH for 10 min. Separation of acidic sugars was performed by using 150 mM NaOAc and 100 mM NaOH for 10 min at a flow rate of 1 mL/min at 40°C. Standard curves of neutral sugars (D-Fuc, L-Rha, L-Ara, D-Gal, D-Glc, D-Xyl, and D-Man) or acidic sugars (D-GalA and D-GlcA) were used for quantitation.

**Leaf-shape analysis**

Rosettes from 4-week old plants grown under long day condition were detached and photographed immediately. Leaves were removed from the rosette and adhered to white paper and then scanned (Epson Perfection V700 scanner). The $8^{th}$ leaf was used for calculation. Blade length, width, perimeter, area, serration number and serration levels were calculated from silhouettes using ImageJ software. Leaf-serration levels are expressed as the distance from tip-to-midvein divided by the distance from sinus-to-midvein, for indicated tooth ($2^{nd}$-$4^{th}$) (Kawamura *et al.*, 2010).

**Stomatal aperture**

The stomatal aperture measurement was performed according to Distéfano et al., (2012) with minor modifications. The stomatal aperture treatments were performed on epidermal strips excised from the abaxial side of fully expanded Arabidopsis leaves. Epidermal peels from leaves of 3-week-old plants, grown at 22°C under 16 h of light and 8h of dark, were stripped and immediately floated in opening buffer (5 mM MES-KOH (pH 6.1), 50 mM KCl) for 3 h. The strips were subsequently maintained in the same opening buffer and exposed to different ABA concentration. After 90 min, stomata were digitized using a Nikon DS-Fi 1 camera, coupled to a Nikon Eclipse Ti microscope. The stomatal-aperture width was measured using ImageJ software (National Institute of Health).

**$^{32}$Pi-phospholipid labelling, extraction and analysis**

Developing seeds at 10 DAP were carefully removed from silique. Mature seeds were sterilized and stratified on ½MS (pH 5.8) as described and germinated under long day conditions for around 20 h when testa ruptured. Both developing and germinating seeds were then transferred to 200 µl labeling buffer (2.5 mM MES, pH 5.8, 1 mM KCl) containing 5-10 µCi $^{32}PO_4^{3-}$ ($^{32}P_i$) (carrier free; Perklin-Elmer) in a 2 ml Eppendorf, Safelock microcentrifuge tube for 24 h.

Five-day-old seedlings were labeled similarly, except for 3 h labeling time. Samples were treated by adding 200 µl labeling buffer with or without 600 mM sorbitol for 30 mins.

Labeling an subsequent treatments were stopped by adding perchloric acid (final concentration, 5% by vol.) for 5-10 min, after which lipids were extracted and the phosphoinositides and PA separated from the rest of the phospholipids by thin-layer chromatography (TLC) as described in detail by Munnik & Zarza (2013). Radioactive phospholipids were visualized by autoradiography and quantified by phosphoimaging (Molecular Dynamics, Sunnyvale, CA, USA). Individual phospholipid levels are expressed as the percentage of the total $^{32}$P-lipid fraction.

## Drought tolerance assays

Drought assay were performed as described previously (Hua *et al.*, 2012; Osakabe *et al.*, 2013) with some changes. Seeds were stratified at 4°C in the dark and sowed in soil pots (4.5 cm x 4.5 cm x 7.5 cm) containing equal amounts (80 g) of soil. Nine plants per pot were grown under short-day conditions (22 °C with 12 h light/12 h dark) for 4 weeks, and then subjected to dehydration by withholding them for water for 2 weeks, while control plants were normally watered. At this point, plants were photographed. Each experiment used 36 plants per genotype and experiments were repeated at least 3 times.

To assay water-loss, rosettes from 4-week-old plants were detached and FW determined every hour by weighing. Water content was calculated as the percentage from the initial FW. Twenty plants were used for each experiment, which was repeated at least 3 times.

**ACKNOWLEDGEMENTS**

This work was financially supported by the China Scholarship Council (CSC File No. 201206300058 to Q.Z) and by the Netherlands Organization for Scientific Research (NWO; 867.15.020 to T.M.).

**REFERENCES**

Allen GJ, and Sanders D (1994) Osmotic stress enhances the competence of Beta vulgaris vacuoles to respond to inositol 1,4,5-trisphosphate. *Plant J* **6**:687–695.

Anderson CT, Carroll A, Akhmetova L, and Somerville C (2010) Real-Time Imaging of Cellulose Reorientation during Cell Wall Expansion in Arabidopsis Roots. *Plant Physiol* **152**:787–796.

Arisz SA, Testerink C, and Munnik T (2009) Plant PA signaling via diacylglycerol kinase. *Biochim Biophys Acta* **1791**:869–875.

Arisz SA, van Wijk R, Roels W, Zhu JK, Haring MA, and Munnik T (2013) Rapid phosphatidic acid accumulation in response to low temperature stress in Arabidopsis is generated through diacylglycerol kinase. *Front Plant Sci* **4**:1–15.

Balla T (2013) Phosphoinositides: tiny lipids with giant impact on cell regulation. *Physiol Rev* **93**:1019–1137.

Basu D, Tian L, DeBrosse T, Poirier E, Emch K, Herock H, Travers A, and Showalter AM (2016) Glycosylation of a Fasciclin-Like Arabinogalactan-Protein (SOS5) mediates root growth and seed mucilage adherence via a cell wall receptor-like kinase (FEI1/ FEI2) Pathway in Arabidopsis. *PLoS One* **11**:1–27.

Bauer H, Ache P, Lautner S, Fromm J, Hartung W, Al-Rasheid KAS, Sonnewald S, Sonnewald U, Kneitz S, Lachmann N, Mendel RR, Bittner F, Hetherington AM, and Hedrich R (2013) The stomatal response to reduced relative humidity requires guard cell-autonomous ABA synthesis. *Curr Biol* **23**:53–57.

Ben-Tov D, Abraham Y, Stav S, Thompson K, Loraine A, Elbaum R, de Souza A, Pauly M, Kieber JJ, and Harpaz-Saad S (2015) COBRA-LIKE2, a member of the glycosylphosphatidylinositol-anchored COBRA-LIKE family, plays a role in cellulose deposition in arabidopsis seed coat mucilage secretory cells. *Plant Physiol* **167**:711–24.

Bilsborough GD, Runions A, Barkoulas M, Jenkins HW, Hasson A, and Galinha C (2011) Model for the regulation of Arabidopsis thaliana leaf margin development. *PNAS* **108**:3424–3429.

Blatt MR, Thiel G, and Trentham DR (1990) Reversible inactivation of K+ channels of Vicia stomatal guard cells following the photolysis of caged inositol 1,4,5-trisphosphate. *Nature* **346**:766–769.

Byrne ME (2005) Networks in leaf development. *Curr Opin Plant Biol* **8**:59–66.

Carpita NC, and Gibeaut DM (1993) Structural models of primary cell walls in flowering plants: consistency of molecular structure with the physical properties of the walls during growth. *Plant J* **3**:1–30.

Clough SJ, and Bent AF (1998) Floral dip: A simplified method for Agrobacterium-mediated transformation of Arabidopsis thaliana. *Plant J* **16**:735–743.

Cosgrove DJ (1997) Assembly and enlargement of the primary cell wall in plants. *Annu Rev Cell Dev Biol* **13**:171–201.

D'Ambrosio JM, Couto D, Fabro G, Scuffi1 D, Lamattina L, Munnik T, Álvarez ME, Andersson MX, Zipfel C, and Laxalt AM (2017) Phosphoinositide-specific phospholipase C2 (PLC2)associates with RBOHD and modulates ROS production and MAMP-triggered immunity in Arabidopsis. *Plant J* **submitted**.

Di Fino L, D'Ambrosio J, Tejos R, van Wijk R, Lamattina T, Munnik T, Pagnussat G, and Laxalt AM (2017) Arabidopsis phosphatidylinositol-phospholipase C2 (PLC2) is involved in female gametogenesis and embryo development. *Planta* **2**:1–12.

Distéfano AM, Scuffi D, García-Mata C, Lamattina L, and Laxalt AM (2012) Phospholipase D?? is involved in nitric oxide-induced stomatal closure. *Planta* **236**:1899–1907.

Dowd PE, Coursol S, Skirpan AL, Kao T, and Gilroy S (2006) Petunia phospholipase C1 is involved in pollen tube growth. *Plant Cell* **18**:1438–1453.

Fleming AJ (2005) The control of leaf development. *New Phytol* **166**:9–20.

Gao K, Liu YL, Li B, Zhou RG, Sun DY, and Zheng SZ (2014) Arabidopsis thaliana phosphoinositide-specific phospholipase C isoform 3 (AtPLC3) and AtPLC9 have an additive effect on thermotolerance. *Plant Cell Physiol* **55**:1873–1883.

Georges F, Das S, Ray H, Bock C, Nokhrina K, Kolla VA, and Keller W (2009) Over-expression of Brassica napus phosphatidylinositol-phospholipase C2 in canola induces significant changes in gene expression and phytohormone distribution patterns, enhances drought tolerance and promotes early flowering and maturation. *Plant, Cell Environ* **32**:1664–1681.

Gillaspy GE (2013) The role of phosphoinositides and inositol phosphates in plant cell signaling, in *Lipid-mediated protein signaling* (Capelluto DGS ed) pp 141–157.

Gilroy S, Read ND, and Trewavas a J (1990) Elevation of cytoplasmic calcium by caged calcium or caged inositol triphosphate initiates stomatal closure. *Nature* **346**:769–771.

Han B, Yang Z, Samma MK, Wang R, and Shen W (2013) Systematic validation of candidate reference genes for qRT-PCR normalization under iron deficiency in Arabidopsis. *BioMetals* **26**:403–413.

Harpaz-Saad S, McFarlane HE, Xu S, Divi UK, Forward B, Western TL, and Kieber JJ (2011) Cellulose synthesis via the FEI2 RLK/SOS5 pathway and CELLULOSE SYNTHASE 5 is required for the structure of seed coat mucilage in Arabidopsis. *Plant J* **68**:941–953.

Hay A, Barkoulas M, and Tsiantis M (2006) ASYMMETRIC LEAVES1 and auxin activities converge to repress BREVIPEDICELLUS expression and promote leaf development in Arabidopsis. *Development* **133**:3955–3961.

Hay A, and Tsiantis M (2006) The genetic basis for differences in leaf form between Arabidopsis thaliana and its wild relative Cardamine hirsuta. *Nat Genet* **38**:942–947.

Heilmann I (2016) Phosphoinositide signaling in plant development. *Development* **143**:2044–2055.

Helling D, Possart A, Cottier S, Klahre U, and Kost B (2006) Pollen tube tip growth depends on plasma membrane polarization mediated by tobacco PLC3 activity and endocytic membrane recycling. *Plant Cell* **18**:3519–3534.

Hou Q, Ufer G, and Bartels D (2016) Lipid signalling in plant responses to abiotic stress. *Plant, Cell Environ* **39**:1029–1048.

Hu R, Li J, Wang X, Zhao X, Yang X, Tang Q, He G, Zhou G, and Kong Y (2016) Xylan synthesized by Irregular Xylem 14 (IRX14) maintains the structure of seed coat mucilage in Arabidopsis. *J Exp Bot* **67**:1243–1257.

Hu R, Li J, Yang X, Zhao X, Wang X, Tang Q, He G, Zhou G, and Kong Y (2016) Irregular xylem 7 (IRX7) is required for anchoring seed coat mucilage in Arabidopsis. *Plant Mol Biol* **92**:25–38.

Hua D, Wang C, He J, Liao H, Duan Y, Zhu Z, Guo Y, Chen Z, and Gong Z (2012) A plasma membrane receptor kinase, GHR1, mediates abscisic acid- and hydrogen peroxide-regulated stomatal movement in Arabidopsis. *Plant Cell* **24**:2546–61.

Hunt L, and Gray JE (2001) ABA signalling: A messenger's FIERY fate. *Curr Biol* **11**:968–970.

Hunt L, Mills LN, Pical C, Leckie CP, Aitken FL, Kopka J, Mueller-Roeber B, McAinsh MR, Hetherington AM, and Gray JE (2003) Phospholipase C is required for the control of stomatal aperture by ABA. *Plant J* **34**:47–55.

Irvine RF (2006) Nuclear inositide signalling-expansion, structures and clarification. *Biochim Biophys Acta* **1761**:505–508.

Ischebeck T, Werner S, Krishnamoorthy P, Lerche J, Meijón M, Stenzel I, Löfke C, Wiessner T, Im YJ, Perera IY, Iven T, Feussner I, Busch W, Boss WF, Teichmann T, Hause B, Persson S, and Heilmann I (2013) Phosphatidylinositol 4,5-bisphosphate influences PIN polarization by controlling clathrin-mediated membrane trafficking in Arabidopsis. *Plant Cell* **25**:4894–4911.

Kawamura E, Horiguchi G, and Tsukaya H (2010) Mechanisms of leaf tooth formation in Arabidopsis. *Plant J* **62**:429–441.

Kuo HF, Chang TY, Chiang SF, Wang W Di, Charng YY, and Chiou TJ (2014) Arabidopsis inositol pentakisphosphate 2-kinase, AtIPK1, is required for growth and modulates phosphate homeostasis at the transcriptional level. *Plant J* **80**:503–515.

Laha D, Johnen P, Azevedo C, Dynowski M, Weiß M, Capolicchio S, Mao H, Iven T, Steenbergen M, Freyer M, Gaugler P, de Campos MKF, Zheng N, Feussner I, Jessen HJ, Van Wees SCM, Saiardi A, and Schaaf G (2015) VIH2 regulates the synthesis of inositol pyrophosphate InsP8 and jasmonate-dependent defenses in Arabidopsis. *Plant Cell* **27**:1082–1097.

Laha D, Parvin N, Dynowski M, Johnen P, Mao H, Bitters ST, Zheng N, and Schaaf G (2016) Inositol polyphosphate binding specificity of the jasmonate receptor complex. *Plant Physiol* **171**:2364–2370.

Lee HS, Lee DH, Cho HK, Kim SH, Auh JH, and Pai HS (2015) InsP6-sensitive variants of the Gle1 mRNA export factor rescue growth and fertility defects of the ipk1 low-phytic-acid mutation in Arabidopsis. *Plant Cell* **27**:417–431.

Lemtiri-Chlieh F, MacRobbie EAC, and Brearley CA (2000) Inositol hexakisphosphate is a physiological signal regulating the K+-inward rectifying conductance in guard cells. *Proc Natl Acad Sci U S A* **97**:8687–8692.

Lemtiri-Chlieh F, MacRobbie EAC, Webb AAR, Manison NF, Brownlee C, Skepper JN, Chen J, Prestwich GD, and Brearley CA (2003) Inositol hexakisphosphate mobilizes an endomembrane store of calcium in guard cells. *Proc Natl Acad Sci U S A* **100**:10091–10095.

Li J, Pleskot R, Henty-Ridilla JL, Blanchoin L, Potocký M, and Staiger CJ (2012) Arabidopsis capping protein senses cellular phosphatidic acid levels and transduces these into changes in actin cytoskeleton dynamics. *Plant Signal Behav* **7**:1727–1730.

Li L, He Y, Wang Y, Zhao S, Chen X, Ye T, Wu Y, and Wu Y (2015) Arabidopsis PLC2 is involved in auxin-modulated reproductive development. *Plant J* **84**:504–515.

Li M, Hong Y, and Wang X (2009) Phospholipase D- and phosphatidic acid-mediated signaling in plants. *Biochim Biophys Acta - Mol Cell Biol Lipids* **1791**:927–935.

Liu Y, Su Y, and Wang X (2013) Phosphatidic Acid-Mediated Signaling, in *Lipid-mediated Protein Signaling* (Capelluto DGS ed) pp 159–176.

Macquet A, Ralet MC, Kronenberger J, Marion-Poll A, and North HM (2007) In situ, chemical and macromolecular study of the composition of Arabidopsis thaliana seed coat mucilage. *Plant Cell Physiol* **48**:984–999.

Martin TF. (2001) PI(4,5)P2 regulation of surface membrane traffic. *Curr Opin Cell Biol* **13**:493–499.

Meijer HJG, van Himbergen JAJ, Musgrave A, and Munnik T (2017) Acclimation to salt modifies the activation of several osmotic stress-activated lipid signalling pathways in Chlamydomonas. *Phytochemistry* **135**:64–72.

Mendu V, Griffiths JS, Persson S, Stork J, Downie AB, Voiniciuc C, Haughn GW, and DeBolt S (2011) Subfunctionalization of Cellulose Synthases in Seed Coat Epidermal Cells Mediates Secondary Radial Wall Synthesis and Mucilage Attachment. *Plant Physiol* **157**:441–453.

Michell RH (2008) Inositol derivatives: evolution and functions. *Nat Rev* **9**:151–161.

Monserrate JP, and York JD (2010) Inositol phosphate synthesis and the nuclear processes they affect. *Curr Opin Cell Biol* **22**:365–373.

Mosblech A, König S, Stenzel I, Grzeganek P, Feussner I, and Heilmann I (2008) Phosphoinositide and inositolpolyphosphate signalling in defense responses of Arabidopsis thaliana challenged by mechanical wounding. *Mol Plant* **1**:249–261, The Authors 2007. All rights reserved.

Mosblech A, Thurow C, Gatz C, Feussner I, and Heilmann I (2011) Jasmonic acid perception by COI1 involves inositol polyphosphates in Arabidopsis thaliana. *Plant J* **65**:949–957.

Mueller-roeber B, and Pical C (2002) Inositol phospholipid metabolism in Arabidopsis . characterized and putative isoforms of inositol phospholipid kinase and phosphoinositide-specific phospholipase C. *Plant Physiol* **130**:22–46.

Munnik T (2014) PI-PLC: Phosphoinositide-phospholipase C in plant signalling, in *Phospholipases in Plant Signaling* (Wang X ed) pp 27–54.

Munnik T, and Nielsen E (2011) Green light for polyphosphoinositide signals in plants. *Curr Opin Plant Biol* **14**:489–497.

Munnik T, and Testerink C (2009) Plant phospholipid signaling: "in a nutshell". *J Lipid Res* **50**:S260–S265.

Munnik T, and Vermeer JEM (2010) Osmotic stress-induced phosphoinositide and inositol phosphate signalling in plants. *Plant Cell Environ* **33**:655–669.

Murphy AM, Otto B, Brearley CA, Carr JP, and Hanke DE (2008) A role for inositol hexakisphosphate in the maintenance of basal resistance to plant pathogens. *Plant J* **56**:638–652.

Nikovics K, Blein T, Peaucelle A, Ishida T, Morin H, Aida M, and Laufs P (2006) The balance between the MIR164A and CUC2 genes controls leaf margin serration in Arabidopsis. *Plant Cell* **18**:2929–2945.

Osakabe Y, Arinaga N, Umezawa T, Katsura S, Nagamachi K, Tanaka H, Ohiraki H, Yamada K, Seo S-U, Abo M, Yoshimura E, Shinozaki K, and Yamaguchi-Shinozaki K (2013) Osmotic stress responses and plant growth controlled by potassium transporters in Arabidopsis. *Plant Cell* **25**:609–624.

Pieterse CMJ (1998) A novel signaling pathway controlling induced systemic resistance in Arabidopsis. *Plant Cell* **10**:1571–1580.

Pleskot R, Li J, Žárský V, Potocký M, and Staiger CJ (2017) Regulation of cytoskeletal dynamics by phospholipase D and phosphatidic acid. *Trends Plant Sci* **18**:496–504.

Pleskot R, Potocký M, Pejchar Př, Linek J, Bezvoda R, Martinec J, Valentová O, Novotná Z, and Žárský V (2010) Mutual regulation of plant phospholipase D and the actin cytoskeleton. *Plant J* **62**:494–507.

Pokotylo I, Kolesnikov Y, Kravets V, Zachowski A, and Ruelland E (2014) Plant phosphoinositide-dependent phospholipases C: Variations around a canonical theme. *Biochimie* **96**:144–157.

Puga MI, Mateos I, Charukesi R, Wang Z, Franco-Zorrilla JM, de Lorenzo L, Irigoyen ML, Masiero S, Bustos R, Rodríguez J, Leyva A, Rubio V, Sommer H, and Paz-Ares J (2014) SPX1 is a phosphate-dependent inhibitor of Phosphate Starvation Response 1 in Arabidopsis. *Proc Natl Acad Sci U S A* **111**:14947–14952.

Repp A, Mikami K, Mittmann F, and Hartmann E (2004) Phosphoinositide-specific phospholipase C is involved in cytokinin and gravity responses in the moss Physcomitrella patens. *Plant J* **40**:250–259.

Saez-Aguayo S, Rautengarten C, Temple H, Sanhueza D, Ejsmentewicz T, Sandoval-Ibañez O, Doñas-Cofré DA, Parra-Rojas JP, Ebert B, Lehner A, Mollet J-C, Dupree P, Scheller H V., Heazlewood JL, Reyes FC, and Orellana A (2017) UUAT1 Is a Golgi-Localized UDP-Uronic Acid Transporter that Modulates the Polysaccharide Composition of Arabidopsis Seed Mucilage. *Plant Cell* doi:10.1105.

Saez-Aguayo S, Rondeau-Mouro C, Macquet A, Kronholm I, Ralet MC, Berger A, Sallé C, Poulain D, Granier F, Botran L, Loudet O, de Meaux J, Marion-Poll A, and North HM (2014) Local Evolution of Seed Flotation in Arabidopsis. *PLoS Genet* **10**:13–15.

Sanchez JP, and Chua NH (2001) Arabidopsis PLC1 is required for secondary responses to abscisic acid signals. *Plant Cell* **13**:1143–1154.

Scarpella E, Marcos D, Friml J, Berleth T, Scarpella E, Marcos D, and Berleth T (2006) Control of leaf vascular patterning by polar auxin transport Control of leaf vascular patterning by polar auxin transport. 1015–1027.

Sean R, Pedro L, Ruth R, and Suzanne R (2010) Abscisic acid:emergence of a core signaling network. *Annu Rev Plant Biol* **61**:651–679.

Sheard LB, Tan X, Mao H, Withers J, Ben-Nissan G, Hinds TR, Kobayashi Y, Hsu F-F, Sharon M, Browse J, He SY, Rizo J, Howe GA, and Zheng N (2010) Jasmonate perception by inositol-phosphate-potentiated COI1-JAZ co-receptor. *Nature* **468**:400–405, Nature Publishing Group, a division of Macmillan Publishers Limited. All Rights Reserved.

Song M, Liu S, Zhou Z, and Han Y (2008) TfPLC1, a gene encoding phosphoinositide-specific phospholipase C, is predominantly expressed in reproductive organs in Torenia fournieri. *Sex Plant Reprod* **21**:259–267.

Stevenson JM, Perera IY, Heilmann I, Persson S, and Boss WF (2000) Inositol signaling and plant growth. *Trends Plant Sci* **5**:252–258.

Sullivan S, Ralet MM-C, Berger A, Diatloff E, Bischoff V, Gonneau M, Marion-Poll A, and North HM (2011) CESA5 is required for the synthesis of cellulose with a role in structuring the adherent mucilage of Arabidopsis seeds. *Plant Physiol* **156**:1725–39.

Tan X, Calderon-Villalobos LI a, Sharon M, Zheng C, Robinson C V, Estelle M, and Zheng N (2007) Mechanism of auxin perception by the TIR1 ubiquitin ligase. *Nature* **446**:640–645.

Tasma IM, Brendel V, Whitham S a., and Bhattacharyya MK (2008) Expression and evolution of the phosphoinositide-specific phospholipase C gene family in Arabidopsis thaliana. *Plant Physiol Biochem* **46**:627–637.

Tejos R, Sauer M, Vanneste S, Palacios-Gomez M, Li H, Heilmann M, van Wijk R, Vermeer JEM, Heilmann I, Munnik T, and Friml J (2014) Bipolar Plasma Membrane Distribution of Phosphoinositides and Their Requirement for Auxin-Mediated Cell Polarity and Patterning in Arabidopsis. *Plant Cell* **26**:2114–2128.

Testerink C, and Munnik T (2011) Molecular, cellular, and physiological responses to phosphatidic acid formation in plants. *J Exp Bot* **62**:2349–2361.

Thomas C, and Staiger CJ (2014) A dynamic interplay between membranes and the cytoskeleton critical for cell development and signaling. *Front Plant Sci* **5**:335.

Thota SG, and Bhandari R (2015) The emerging roles of inositol pyrophosphates in eukaryotic cell physiology. *J Biosci* **40**:593–605.

Tripathy MK, Tyagi W, Goswami M, Kaul T, Singla-Pareek SL, Deswal R, Reddy MK, and Sopory SK (2011) Characterization and Functional Validation of Tobacco PLC Delta for Abiotic Stress Tolerance. *Plant Mol Biol Report* **30**:488–497.

Tsukaya H (2006) Mechanism of leaf-shape determination. *Annu Rev Plant Biol* **57**:477–496.

Tsukaya H, and Uchimiya H (1997) Genetic analyses of the formation of the serrated margin of leaf blades in Arabidopsis: Combination of a mutational analysis of leaf morphogenesis with the characterization of a specific marker gene expressed in hydathodes and stipules. *Mol Gen Genet* **256**:231–238.

van Leeuwen W, Vermeer JEM, Gadella TWJ, and Munnik T (2007) Visualization of phosphatidylinositol 4,5-bisphosphate in the plasma membrane of suspension-cultured tobacco BY-2 cells and whole Arabidopsis seedlings. *Plant J* **52**:1014–1026.

Voiniciuc C, Schmidt MH-W, Berger A, Yang B, Ebert B, Scheller H V., North HM, Usadel B, and Günl M (2015) MUCILAGE-RELATED10 Produces Galactoglucomannan That Maintains Pectin and Cellulose Architecture in Arabidopsis Seed Mucilage. *Plant Physiol* **169**:403–420.

Voiniciuc C, Yang B, Schmidt MH-W, Günl M, and Usadel B (2015) Starting to gel: how Arabidopsis seed coat epidermal cells produce specialized secondary cell walls. *Int J Mol Sci* **16**:3452–3473.

Vossen JH, Abd-El-Haliem A, Fradin EF, Van Den Berg GCM, Ekengren SK, Meijer HJG, Seifi A, Bai Y, Ten Have A, Munnik T, Thomma BPHJ, and Joosten MHAJ (2010) Identification of tomato phosphatidylinositol-specific phospholipase-C (PI-PLC) family members and the role of PLC4 and PLC6 in HR and disease resistance. *Plant J* **62**:224–239.

Wallace IS, and Anderson CT (2012) Small Molecule Probes for Plant Cell Wall Polysaccharide Imaging. *Front Plant Sci* **3**:1–8.

Wang CR, Yang AF, Yue GD, Gao Q, Yin HY, and Zhang JR (2008) Enhanced expression of phospholipase C 1 (ZmPLC1) improves drought tolerance in transgenic maize. *Planta* **227**:1127–1140.

Wang X, Devaiah SP, Zhang W, and Welti R (2006) Signaling functions of phosphatidic acid. *Prog Lipid Res* **45**:250–278.

Western TL, Skinner DJ, and Haughn GW (2000) Differentiation of mucilage secretory cells of the Arabidopsis seed coat. *Plant Physiol* **122**:345–356.

Wheeler GL, and Brownlee C (2008) Ca2+ signalling in plants and green algae - changing channels. *Trends Plant Sci* **13**:506–514.

Wild R, Gerasimaite R, Jung J-Y, Truffault V, Pavlovic I, Schmidt A, Saiardi A, Jessen HJ, Poirier Y, Hothorn M, and Mayer A (2016) Control of eukaryotic phosphate homeostasis by inositol polyphosphate sensor domains. *Science (80- )* **352**:986 LP-990.

Willats WGT, Mccartney L, and Knox JP (2001) Pectinas Polissacarideos.

Williams SP, Gillaspy GE, and Perera IY (2015) Biosynthesis and possible functions of inositol pyrophosphates in plants. *Front Plant Sci* **6**:1–12.

Yu L, Shi D, Li J, Kong Y, Yu Y, Chai G, Hu R, Wang J, Hahn MG, and Zhou G (2014) CELLULOSE SYNTHASE-LIKE A2, a glucomannan synthase, is involved in maintaining adherent mucilage structure in Arabidopsis seed. *Plant Physiol* **164**:1842–1856.

Zheng S, Liu Y, Li B, Shang Z, Zhou R, and Sun D (2012) Phosphoinositide-specific phospholipase C9 is involved in the thermotolerance of Arabidopsis. *Plant J* **69**:689–700.

SUPPLEMENTAL DATA

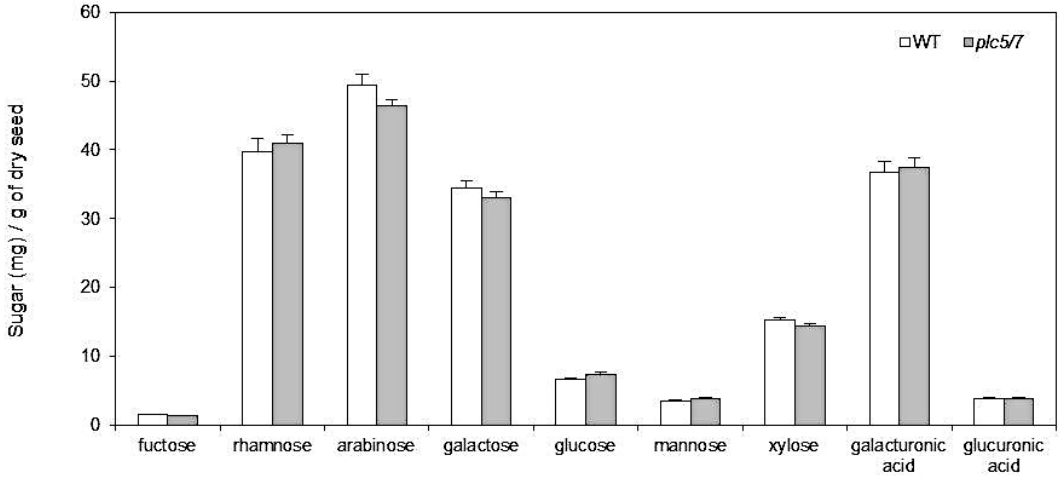


**Supplemental Figure S1.** Sugar composition of wild type- and *plc5/7*-mutant seeds.Sugars were extracted from dry seeds and quantified by HPAEC-PAD. Quantities were corrected through internal standards, and transformed into mg of sugar per gram of dry material. Values represent the means of triplicates ± SE of three independent experiments.

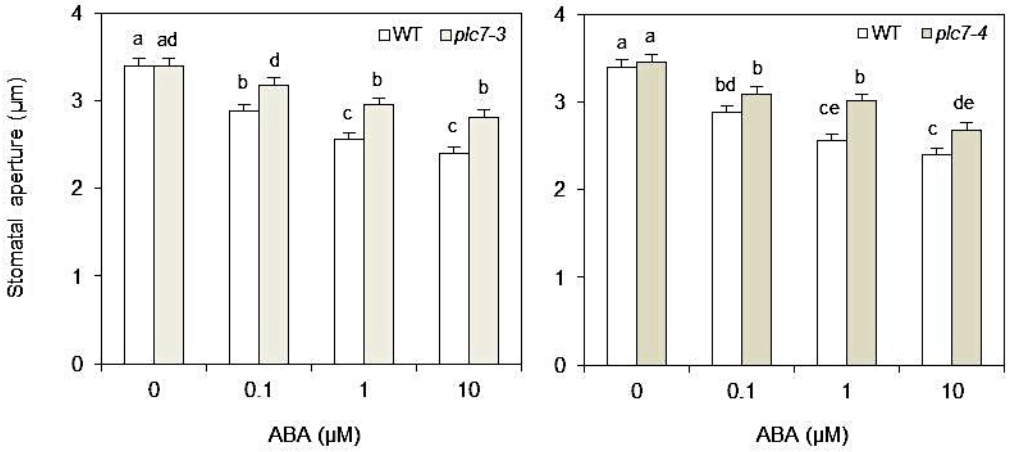


**Supplemental Figure S2.** Decreased ABA sensitivity of *plc7* mutants in stomatal closure.
Leaves from 3-weeks old plants were stripped and peels were incubated in opening buffer with light for 3 h until stomata were fully open. Peels were then treated with different concentrations of ABA for 90 mins, after which stomata were digitized and the aperture width measured for wild type and *plc7-3* (left) or *plc7-4* (right). Values are means ± SE of at least three independents (n >100). Data was analyzed by 2-way ANOVA. Statistical significant differences between genotypes are indicated by letters ($P<0.05$, Dunn's method).